Supplementary information

for

Optically Switchable CLEAR Probes Enable Rapid, Biocompatible and High-Efficiency Fluorophore Exchange for Ultra-Plex, High-Resolution Immunofluorescence Imaging

Simanta Kalita,[a] Pratibha Kumari,[a] Arka Som,[a] Srishti Mandal,[b] Resmi V. Nair,[a] Saswata Bandyopadhyay,[a] Sushma S. Rao,[c] Sudha Kumari,[b] and Sarit S. Agasti [a]*

[a] Simanta Kalita, Dr. Pratibha Kumari, Dr. Arka Som, Dr. Resmi V. Nair, Saswata Bandyopadhyay, Prof. Sarit S. Agasti
New Chemistry Unit and Chemistry & Physics of Materials Unit, School of Advanced Materials (SAMat)
Jawaharlal Nehru Centre for Advanced Scientific Research (JNCASR), Bangalore, Karnataka 560064, India
E-mail: sagasti@jncasr.ac.in

[b] Srishti Mandal, Dr. Sudha Kumari
Department of Microbiology and Cell Biology, Indian Institute of Science (IISc), Bangalore, Karnataka 560012, India

[c] Sushma S. Rao
Neuroscience Unit, Jawaharlal Nehru Centre for Advanced Scientific Research (JNCASR), Bangalore, Karnataka 560064, India

A. General: materials and methods

All the chemicals were purchased from either of the following companies: Sigma-Aldrich (part of MilliporeSigma), Thermo Fisher Scientific, TCI chemicals, SD fine chemicals, and Spectrochem, unless mentioned specifically. Amino phalloidin was purchased from the American Peptide Company (Product No. 92-1-10). Zeba™ spin desalting columns were purchased from Thermo Fisher Scientific. Antibodies and dyes were purchased from commercial sources as listed in the sections below. Whenever necessary, solvents were dried by using standard solvent drying methods and used for reactions. Yields were calculated either from the actual isolated mass of the product or by quantification of the product peak area in HPLC chromatogram. ^{1}H NMR spectra were recorded using Bruker ADVANCE III 400 MHz instrument and JEOL 600 MHz instrument. NMR spectra were processed and analyzed using the MestreNova software package. High-Resolution Mass Spectrometry (HRMS) was carried out using Agilent 6538 Ultra High Definition (UHD) Accurate-Mass Q-TOF

LC/MS. Liquid Chromatography Mass Spectrometry (LC-MS) was carried out using the Waters e2695 instrument. High-Performance Liquid Chromatography (HPLC) purification was carried out using Agilent 1260 infinity quaternary HPLC system equipped with analytical XTerra MS C18 column (4.6 mm (internal diameter) × 50 mm (length), particle size 5 µm, 100Å pore size) and semi-preparative Luna C18 column (250 mm (length) × 10 mm (internal diameter), particle size 5 µm, 100Å pore size). The solvents, used as eluent in HPLC purification, were solvent A (water containing 0.1% TFA) and solvent B (acetonitrile containing 0.1% TFA). Semi-preparative scale High-Performance Liquid Chromatography was performed utilising a Waters preparative HPLC system equipped with a Waters 1525 binary HPLC pump and Waters2489 UV-Visible detector with XTerra Prep MS C18 OBD column (50 mm (length) × 19 mm (internal diameter), particle size 5 µm, 125 Å pore size). Absorbance measurements for calculating concentrations of the fluorophore conjugates were done using BioSpectrometer (Eppendorf). The concentrations of antibody conjugates were measured using the NanoDrop One instrument (Thermo Fisher Scientific). Photocleavage and fluorescence signal-erasing experiments were carried out using a 365 nm LED system (CS2010, Thorlabs)

An inverted Zeiss ELYRA PS1 microscope was used for acquiring all the widefield images, including the dSTORM super-resolved images. Three LASERs were used for the experiments: 488 (20 mW at the sample plane), 561 nm (36 mW at the sample plane), and 642 nm (22 mW at the sample plane). All the widefield imaging was performed either by using Zeiss oil–immersion Plan–apochromat DIC 63×/1.40 Oil DIC M27, numerical aperture (NA) 1.40 oil objective or alpha Plan-apochromat DIC 100×/1.46 Oil DIC M27, NA 1.46 objectives. The images were acquired using an electron-multiplying charge-coupled device (EMCCD) camera (Andor iXon DU897, quantum yield > 90 %, 512 × 512 pixels). Fluorescence light was spectrally filtered with emission filters MBS-488+EF BP 495-575/ LP 750 for 488 nm LASER, MBS–561+EF BP 570–650/LP 750 for 561 nm LASER and MBS–642+EF LP 655 for 642 nm LASER. The EMCCD gain was varied for every target protein, depending on the intensity of that protein in the image, and the exposure time was kept at 100 ms for the images other than the dSTORM images.

Confocal imaging studies were performed in a Leica TCS SP8 confocal microscope. For various experiments, a total of four LASERS of wavelengths 405 nm (source: 50 mW), 488 nm (source: 20 mW), 552 nm (source: 20 mW), and 638 nm (source: 30 mW) were used. All the images were acquired using a HyD detector while maintaining an appropriate line average parameter and 400 Hz scanning speed.

Fluorescence lifetime measurements were carried out using a Horiba DeltaFlex time-correlated single-photon counting (TCSPC) system (for the AZ647 dye) and an Edinburgh FLS1000 spectrometer (for the AZ488 and AZ568 dyes).

Supplementary Table 1: *List of primary antibodies used in this study*

Target	Antibody Species	Commercial source
Microtubule (α-tubulin)	Rat	Thermo Fisher Scientific (MA1-80017)
Mitochondria (TOM-20)	Mouse/Rabbit	Santa Cruz Biotechnology (sc-17764)/ Santa Cruz Biotechnology (sc-11415)
EGFR (Cetuximab)	Human	Merck
Cytokeratin 18	Rabbit	Proteintech (10830-1-AP)
ZAP70	Rabbit	Cell Signalling Technology (2701)
NUP98	Rat	Abcam (ab50610)
Acetylated tubulin	Mouse	Sigma (T7451)
Clathrin	Mouse	Thermo Fisher Scientific (MA1-065)
Lamin B1	Rabbit	Abcam (ab16048)
Paxillin	Sheep	R&D systems (AF4259)
Vimentin	Mouse	Sigma (V6389)
CD45R	Rat	Thermo Fisher Scientific CD45R (B220) (RA3-6B2)
CD4-Alexa Fluor647	Rat	Biolegend (100426)

Supplementary Table 2: *Small molecule and other miscellaneous targeting agents*

Target	Targeting agent	Commercial Source
Glycoprotein and glycolipids	WGA-FITC	Merck (L4895)

Actin	Phalloidin	American Peptide Company (92-1-10)

Supplementary Table 3: *List of secondary antibodies that are used in this study*

Target Species	Host	Specification & Commercial Source
Rat	Donkey	Donkey Anti-Rat IgG (H+L) Jackson ImmunoResearch Laboratories Inc. (Cat. No. 712-005-153)
Rabbit	Donkey	Donkey Anti-Rabbit IgG (H+L) Jackson ImmunoResearch Laboratories Inc. (Cat. No. 711-005-152)
Human	Donkey	Dockey Anti-Human IgG (H+L) Jackson ImmunoResearch Laboratories Inc. (Cat. No. 709-005-149)
Mouse	Donkey	Donkey Anti-Mouse IgG (H+L) Jackson ImmunoResearch Laboratories Inc. (Cat. No. 715-005-151)
Sheep	Donkey	Donkey Anti-Sheep IgG (H+L) Jackson ImmunoResearch Laboratories Inc. (Cat. No. - 713-005-003)

Supplementary Table 4: *List of fluorophore NHS esters that are used to prepare CLEAR probes*

Fluorophore	Commercial Source
AZdye488 NHS ester	Fluoroprobe (1013-5)
AZDye568 NHS ester	Fluoroprobe (1081-5)
AZDye647 NHS ester	Fluoroprobe (1121-5)

B. Synthesis of cleavable linker and CLEAR probes construction

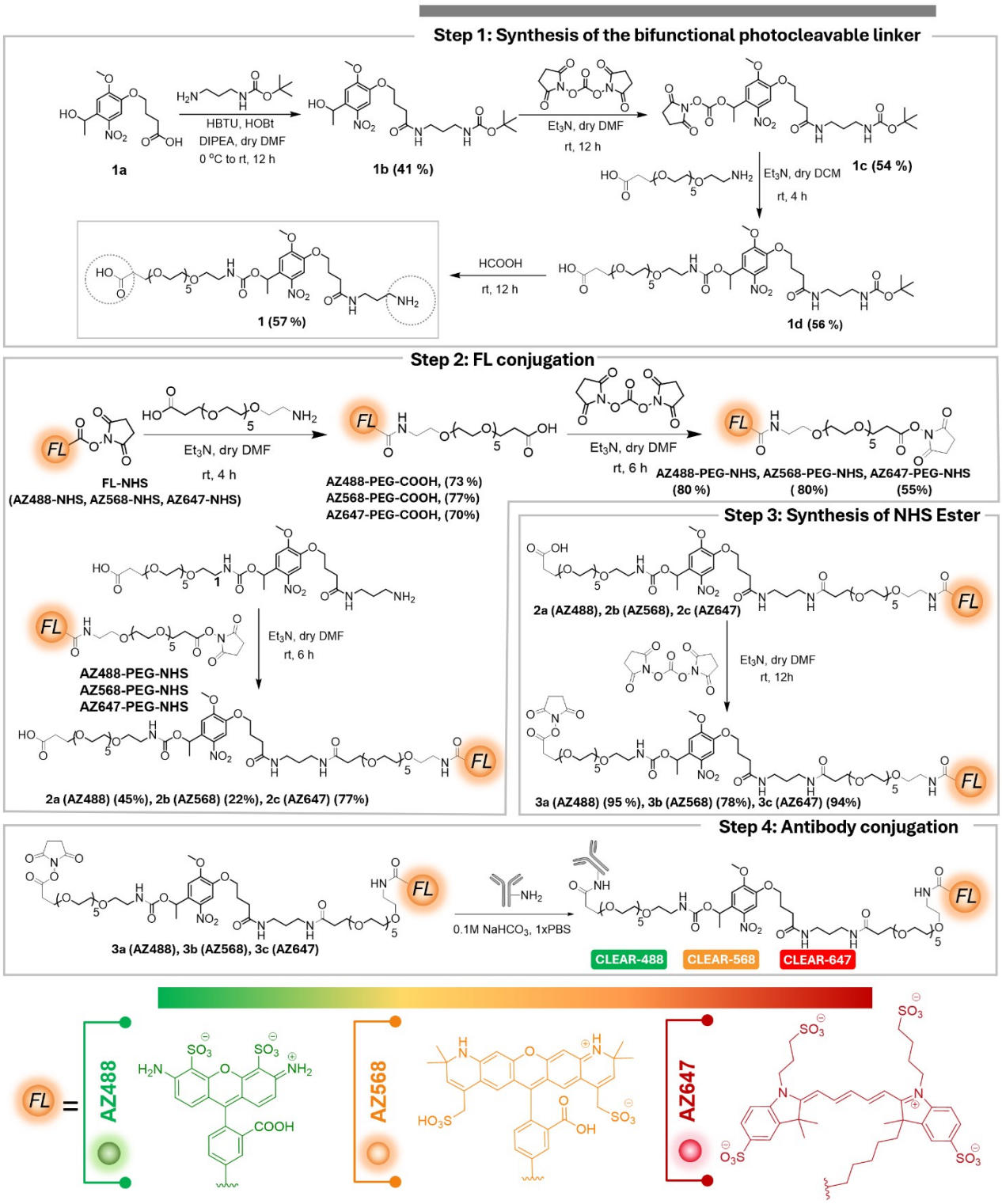

Scheme S1: *Schematic showing the synthetic strategy for preparing spectrally different CLEAR probes that are used for multiplexed imaging. The structures of the fluorophores are shown in the schematic.*

Synthesis of 1a

Compound **1a** was synthesized according to the protocol reported in the literature. [1] The spectroscopic properties of the synthesized compound match those of the one reported in the literature.

Synthesis of 1b

Compound **1a** (4-[4-(1-Hydroxyethyl)-2-methoxy-5-nitrophenoxy]butyric acid) (100 mg, 0.33 mmol) was dissolved in dry DMF (1.5 ml) in a 25 ml round-bottom flask, and it was purged with nitrogen. HBTU (137.24 mg, 0.36 mmol), HOBt (49.05 mg, 0.36 mmol), and DIPEA (139.59 mg, 1.08 mmol) were then added to the flask and stirred for 10 min at 0°C. After 10 min of stirring, N-(tert-Butoxycarbonyl)-1,3-diaminopropane (69 mg, 0.4 mmol) pre-dissolved in 0.5 ml dry DMF was added dropwise to the mixture with stirring. The mixture was stirred for another 10 min at 0°C and then it was allowed to attain room temperature. At room temperature, the mixture was stirred for 12 h. After 12 h, the crude product was purified using reverse-phase semi-preparative High-Performance Liquid Chromatography. A flow of 10 ml/min was used throughout the HPLC run [Solvent: 0.1 % Trifluoroacetic acid (TFA) in water (A), 0.1 % Trifluoroacetic acid (TFA) in acetonitrile (B); gradient: 5 % to 100 % of B within 35 min]. The product was eluted at R_t = 14.2 min (62.5 mg, yield = 41 %). The HPLC chromatogram is shown in the **Fig. S23**. The product fraction was lyophilized and characterized by ^{1}H NMR, ^{13}C NMR, and HRMS. ^{1}H NMR (400 MHz, $CDCl_3$): δ 7.56 (1H, s), δ 7.31 (1H, s), δ 6.37 (1H, br, s), δ 5.57-5.53 (1H, q), δ 4.88 (1H, br, s), δ 4.12-4.09 (2H, t), δ 3.97 (3H, s), δ 3.31-3.26 (2H, m), δ 3.14-3.09 (2H, m), δ 2.44-2.40 (2H, t), δ 2.22-2.15 (2H, m), δ 1.60-1.56 (2H, m), 1.55-1.54 (3H, d), 1.42 (9H, s). ^{13}C NMR ($CDCl_3$,150 MHz): δ 172.59, 156.84, 154.18, 147.07, 139.74, 137.25, 109.28, 108.91, 79.60, 68.70, 65.84, 56.50, 37.17, 36.06, 32.94, 30.34, 28.51, 25.01, 24.43. The ^{1}H and ^{13}C NMR spectra are shown in **Fig. S39** and **Fig. S40**. HRMS (ESI-MS): calculated 478.2160 $[M+Na]^+$, found 478.2129 $[M+Na]^+$.

Synthesis of 1c

Compound **1b** (60 mg, 0.13 mmol) was dissolved in 1 ml of dry DMF in a 25 ml round-bottom flask with stirring. To that stirring solution, Et_3N (263.25 mg, 2.6 mmol) followed by N,N'-Dissuccinimidyl carbonate (666.04 mg, 2.6 mmol) was added. The reaction was incubated for 12 h at room temperature. After 12 h, the crude product was purified using reverse-phase semi-preparative High-Performance Liquid Chromatography. A flow of 4 ml/min was used throughout the run [Solvent: 0.1 % Trifluoroacetic acid (TFA) in water (A), 0.1 % Trifluoroacetic acid (TFA) in acetonitrile (B); gradient: 5 % to 100 % of B within 45 min]. The product was eluted at R_t = 25 min. The product fraction was lyophilized to get a yellow viscous compound (41 mg, yield = 54 %). The HPLC chromatogram is shown in the **Fig. S24.** The product was characterized by LC-MS. LC-MS (ESI-MS): calculated 597.24 $[M+H]^+$, found 597.44 $[M+H]^+$.

Synthesis of 1d

1-amino-3,6,9,12,15,18-hexaoxahenicosan-21-oic acid (53.01 mg, 0.15 mmol) was dissolved in dry DCM (~ 2 ml) and to that, Et_3N (50.63 mg, 0.5 mmol) was added while stirring. The mixture was stirred for 15 min at room temperature. After that, compound **1c** (32 mg, 0.05 mmol) was added to the reaction mixture, and the reaction was continued with stirring for 4 h at room temperature. The crude product was purified using reverse-phase semi-prep High-Performance Liquid Chromatography. A flow of 4 ml/min was used throughout the run [Solvent: 0.1% Trifluoroacetic acid (TFA) in water (A), 0.1 % Trifluoroacetic acid (TFA) in acetonitrile (B); gradient: 5 % to 40 % of B within 20 min, to 50 % of B in 40 min, to 100 % of B in 47 min]. The product was eluted at R_t = 32 min. The HPLC chromatogram is shown in the **Fig. S25.** The product fraction was lyophilized to get a yellow viscous compound (25 mg, yield = 56 %). The product was characterized by ^{1}H NMR, ^{13}C NMR, and HRMS. ^{1}H NMR (600 MHz, d6-DMSO): δ 7.81-7.79 (1H, m), δ 7.52 (1H, s), δ 7.39-7.37 (1H, m), δ 7.09 (1H, s), δ 6.73-6.71 (1H, m), δ 6.08-6.05 (1H, q), δ 4.02-4.00 (2H, t), δ 3.87 (3H, s), δ 3.56-3.53 (2H, t), δ 3.45-3.42 (22H, m), δ 3.05-2.97 (4H, m), δ 2.88-2.85 (2H, m), δ 2.38-2.36 (2H, t), δ 2.20-2.17 (2H, t), δ 1.93-1.88 (2H, m), δ 1.48-1.43 (5H, m), δ 1.32 (9H, s). The ^{1}H NMR spectrum has been shown in **Fig. S41**. ^{13}C NMR (d6-DMSO, 150MHz): δ 174.27, 171.39, 155.59, 155.26, 153.64, 146.80, 143.39, 139.21, 133.40, 108.45, 77.48, 69.79-68.35 (11 PEG carbon atoms), 67.19, 66.42, 56.21, 40.06, 37.65, 36.25, 31.63, 30.74, 29.62, 28.27, 24.71, 21.94. The ^{13}C NMR spectrum is shown in **Fig. S42**. HRMS (ESI-MS): calculated 857.4003 $[M+Na]^+$, found 857.4733 $[M+Na]^+$.

Synthesis of 1

Compound **1d** (21 mg, 0.03 mmol) was taken in a 25 ml round-bottom flask, and to that formic acid (2 ml) was poured while stirring. The deprotection reaction was allowed to continue overnight at room temperature. Later, the formic acid was removed under reduced pressure and then lyophilized to get the deprotected amine compound as a yellow viscous compound (10.5 mg, yield =57 %). The product was characterized by ^{1}H NMR, ^{13}C NMR, and HRMS. ^{1}H NMR (DMSO-d6, 400 MHz): δ 8.07-8.04 (1H, br, m) δ 7.56 (1H, s), δ 7.42-7.39 (1H, m), δ 7.13 (1H, s), δ 6.13-6.08 (1H, q), δ 4.07-4.04 (2H, t), δ 3.91 (3H, s), δ 3.60-3.57 (2H, t), δ 3.49-3.46 (22H, m), δ 3.14-3.06 (4H, m), δ 2.79-2.75 (2H, t), δ 2.43-2.40 (2H, t), δ 2.28-2.24 (2H, t), δ 1.99-1.92 (2H, m), δ 1.71-1.63 (2H, m), δ 1.52-1.51 (3H, d). ^{13}C NMR (DMSO-d6, 150 MHz): δ171.98, 165.32, 157.79, 155.22, 153.63, 146.76, 139.21, 133.43, 108.50, 69.75-69.08 (11 PEG-carbons), 68.32, 67.16, 66.34, 56.21, 40.05, 36.78, 35.55, 34.93, 31.51, 27.49, 24.63, 21.88. The ^{1}H and ^{13}C NMR spectra are shown in **Fig. S43** and **Fig. S44.** HRMS (ESI-MS): calculated 735.3658 $[M+H]^{+}$, found 735.3647 $[M+H]^{+}$.

Synthesis of AZ488-PEG-COOH

1-amino-3,6,9,12,15,18-hexaoxahenicosan-21-oic acid (150 µg, 0.43 µmol) was dissolved in dry DCM (30 µl) in a microcentrifuge tube and triethyl amine (434 µg, 4.3 µmol) was added to it. This mixture was stirred for 10 min at room temperature. AZDye488 NHS ester (**AZ488-NHS,** 180 µg, 18 µl from a 10 µg/µl stock in anhydrous DMSO, 0.28 µmol) was then added to the reaction mixture and stirred for another 4 h at room temperature. The crude product was purified using reverse-phase analytical High-Performance Liquid Chromatography using a 4 ml/min flow rate throughout the run [Solvent: 0.1% Trifluoroacetic acid (TFA) in water (A), 0.1 % Trifluoroacetic acid (TFA) in acetonitrile (B); gradient: 5 % to 50 % of B within 8 min followed by 100% of B in 11 min]. The product eluted at R_t = 7.2 min (yield = 73 %). The HPLC chromatogram is shown in the **Fig. S26.** The product fraction was lyophilized and characterized by HRMS. HRMS (ESI-MS): calculated 870.2056 $[M+H]^{+}$, found 870.2849 $[M+H]^{+}$.

Synthesis of AZ488-PEG-NHS

AZ488-PEG-COOH (140 µg, 0.16 µmol) was dissolved in 30 µl of anhydrous DMF in a microcentrifuge tube and to that, Et_3N (161.6 µg, 1.6 µmol) was added and stirred for 10min at room temperature. N,N'-Disuccinimidyl carbonate (410 µg, 1.6 µmol) was added afterward and the reaction mixture was stirred for 6 h at room temperature. The crude product was purified in reverse-phase analytical High-Performance Liquid Chromatography using a 4 ml/min flow rate throughout the run [Solvent: 0.1 % Trifluoroacetic acid (TFA) in water (A), 0.1 % Trifluoroacetic acid (TFA) in

acetonitrile (B); gradient: 5 % to 22 % of B in 30 min and then 22 % to 100% of B in 35 min]. The product was eluted at R_t = 19.2 min (Yield = 80 %). The HPLC chromatogram is shown in the **Fig. S27.** The product fraction was lyophilized and then directly proceeded towards the next step.

Synthesis of 2a (AZ488)

Compound **1** (177 µg, 0.24 µmol, 17.7 µl from a 10 mg/ml stock in dry DMF) was taken in a microcentrifuge tube. Et_3N (121.5 µg, 1.2 µmol) was added to that and stirred for 10 min at room temperature. **AZ488-PEG-NHS** (115 µg, 0.12 µmol) was added to the reaction mixture afterward and stirred for another 6 h at room temperature. The crude product was purified using reverse-phase analytical High-Performance Liquid Chromatography using a 4 ml/min flow rate throughout the run. The gradient was set as follows: The solvent mixture attains 5 % to 40 % of B in 20 min, and 100 % of B in 24 min. The product was eluted at 14.2 min (Yield: 45 %). The HPLC chromatogram is shown in the **Fig. S28.** The product fraction was lyophilized and characterized by HRMS. HRMS (ESI-MS): Calculated, 1586.5536 $[M+H]^+$, 812.7584 $[M+H+K]^{2+}$ found, 1586.5451 $[M+H]^+$, 812.7499 $[M+H+K]^{2+}$.

Synthesis of 3a (AZ488)

Compound **2a (AZ488)** (70 µg, 0.04 µmol) was dissolved in 30 µl of dry DMF in a microcentrifuge tube and to that, triethylamine (60.75 µg, 0.6 µmol) was added. The mixture was stirred for 10 min at room temperature. Followed by this, N, N'-Disuccinimidyl carbonate (153.7 µg, 0.6 µmol) was added and the reaction was allowed to continue overnight at room temperature. The crude product was purified using reverse-phase analytical HPLC. The flow was kept at 1 ml/min, and the gradient was set as follows: The solvent mixture attains 5 % to 30 % of B in 40 min, to 100 % of B in 44 min. The product was eluted at 36.4 min (Yield: 95 %). The HPLC chromatogram is shown in the **Fig. S29.** The product fraction was lyophilized and later characterized by HRMS. HRMS (ESI-MS): Calculated, 850.8019 $[M+H+NH_4]^{2+}$, found, 850.8003 $[M+H+NH_4]^{2+}$.

Synthesis of AZ568-PEG-COOH

1-amino-3,6,9,12,15,18-hexaoxahenicosan-21-oic acid (116.63 µg, 0.33 µmol) was dissolved in dry DCM (30 µl) in a microcentrifuge tube and triethylamine (161.6 µg, 1.6 µmol) was added to it. This mixture was stirred for 10 min at room temperature. AZDye568 NHS ester (**AZ568-NHS**, 130 µg, 13 µl from a 10 µg/µl stock in anhydrous DMSO, 0.16 µmol) was then added to the reaction mixture and stirred for 6 h. The crude product was purified using reverse-phase analytical HPLC using a 1 ml/min

flow rate throughout the run [Solvent: 0.1 % Trifluoroacetic acid (TFA) in water (A), 0.1 % Trifluoroacetic acid (TFA) in acetonitrile (B); gradient: 5 % to 50 % of B within 25 min followed by 100 % of B in 27 min]. The product was eluted at R_t = 11.6 min (yield = 77 %). The HPLC chromatogram is shown in the **Fig. S31.** The product fraction was lyophilized and characterized by HRMS. HRMS (ESI-MS): calculated 515.6691 $[M+2H]^{2+}$, found 515.6677 $[M+2H]^{2+}$.

Synthesis of AZ568-PEG-NHS

AZ568-PEG-COOH (120 µg, 0.12 µmol) was dissolved in 30 µl of anhydrous DMF in a microcentrifuge tube and to that, Et_3N (182.25 µg, 1.8 µmol) was added and stirred for 10 min at room temperature. N, N'-Disuccinimidyl carbonate (461.11 µg, 1.8 µmol) was added afterward and the reaction mixture was stirred overnight at room temperature. The crude product was purified using reverse-phase analytical HPLC by using a 1 ml/min flow throughout the run [Solvent: 0.1 % Trifluoroacetic acid (TFA) in water (A), 0.1 % Trifluoroacetic acid (TFA) in acetonitrile (B); gradient: 5 % to 35 % of B in 25 min, 100 % of B in 27 min. The product was eluted at R_t = 15.5 min (Yield = 80 %). The HPLC chromatogram is shown in the **Fig. S32.** The product fraction was lyophilised and proceeded directly towards the next step.

Synthesis of 2b

Compound **1** (176.4 µg, 0.24 µmol, 17.6 µl from a 10 mg/ml stock in DMF) was taken in a microcentrifuge tube, and to that, triethylamine (121.5 µg, 1.2 µmol) was added and the mixture was stirred for 10 min at room temperature. After 10 min, **AZ568-PEG-NHS** ester (92 µg, 0.08 µmol) was added to the reaction mixture, and the reaction was allowed to proceed for 6 h at room temperature. Upon completion of the reaction, the crude product was purified using reverse phase HPLC using a flow rate of 4 ml/min throughout the purification run [Solvent: 0.1 % Trifluoroacetic acid (TFA) in water (A), 0.1 % Trifluoroacetic acid (TFA) in acetonitrile (B); gradient: 5 % to 40 % of B within 45 min followed by 100% of B in 47 min). The product was eluted at R_t = 41.3 min (yield = 22 %). The HPLC chromatogram is shown in the **Fig. S33.** The product fraction was lyophilized and characterized by HRMS. HRMS (ESI-MS): calculated 1746.6788 $[M+H]^+$, found 1746.6763 $[M+H]^+$.

Synthesis of 3b (AZ568)

Compound **2b** (**AZ568**) (25 µg, 0.01 µmol) was dissolved in 20 µl of dry DMF in a microcentrifuge tube and triethylamine (15.19 µg, 0.15 µmol) was added to that solution. The mixture was stirred for 10 min at room temperature. After 10 min, N, N'-Disuccinimidyl carbonate (38.43 µg, 0.15 µmol) was

added to the reaction mixture, and the reaction was allowed to go on overnight at room temperature. The crude product was purified using reverse phase HPLC by using a flow rate of 1 ml/min throughout the purification [Solvent: 0.1 % Trifluoroacetic acid (TFA) in water (A), 0.1 % Trifluoroacetic acid (TFA) in acetonitrile (B); gradient: 5 % to 40 % of B within 45 min followed by 100 % of B in 50 min). The product was eluted at R_t = 34.5 min (yield = 78 %). The HPLC chromatogram is shown in the **Fig. S34.** The product fraction was lyophilized and characterized by HRMS. HRMS (ESI-MS): calculated 922.3512 $[M+2H]^{2+}$, found 922.3501 $[M+2H]^{2+}$.

Synthesis of AZ647-PEG-COOH

1-amino-3,6,9,12,15,18-hexaoxahenicosan-21-oic acid (98.95 µg, 0.28 µmol) was dissolved in dry DCM (30 µl) in a microcentrifuge tube and triethylamine (212.63 µg, 2.1 µmol) was added to it. This mixture was stirred for 10 min at room temperature. AZDye647 NHS ester (**AZ647-NHS**, 180 µg, 18 µl from a 10 µg/µl stock in anhydrous DMSO, 0.14 µmol) was then added to the reaction mixture and stirred for 6 h at room temperature. The crude product was purified using reverse-phase HPLC using a 4 ml/min flow rate throughout the run [Solvent: 0.1 % Trifluoroacetic acid (TFA) in water (A), 0.1 % Trifluoroacetic acid (TFA) in acetonitrile (B); gradient: 5 % to 50 % of B within 20 min followed by 100% of B in 23 min]. The product was eluted at R_t = 10.5 min (yield = 70 %). The HPLC chromatogram is shown in the **Fig. S35.** The product fraction was lyophilized and characterized by HRMS. HRMS (ESI-MS): calculated 1208.4005 $[M+H]^+$, found 1208.3991 $[M+H]^+$.

Synthesis of AZ647-PEG-NHS

AZ647-PEG-COOH compound (100 µg, 0.08 µmol) was dissolved in dry DMF (30 µl) in a microcentrifuge tube and Et_3N (162 µg, 1.6 µmol) was added to it. This mixture was stirred for 10 min at room temperature. N, N'-Disuccinimidyl carbonate (409.87 µg, 1.6 µmol) was then added to the reaction mixture and stirred for another 12 h at room temperature. The crude product was purified using reverse-phase HPLC using a 1 ml/min flow rate throughout the run [Solvent: 0.1 % Trifluoroacetic acid (TFA) in water (A), 0.1 % Trifluoroacetic acid (TFA) in acetonitrile (B); gradient: 5 % to 25 % of B within 30 min followed by 100 % of B in 35 min]. The product was eluted at R_t = 20.5 min (yield = 55 %). The HPLC chromatogram is shown in the **Fig. S36.** The product fraction was lyophilized and proceeded directly towards the next step.

Synthesis of 2c (AZ647)

Compound **1** (88 µg, 0.12 µmol, 8.8 µl from a 10 mg/ml stock in DMF) was taken in a microcentrifuge tube, and to that, Et_3N (81 µg, 0.8 µmol) was added and stirred at room temperature for 10 min. After 10 min, **AZ647-PEG-NHS** (50 µg, 0.04 µmol) was added to the reaction mixture, and the reaction was allowed to continue for 4 h at room temperature. The crude product was purified using reverse-phase HPLC using a 1 ml/min flow rate throughout the run [Solvent: 0.1 % Trifluoroacetic acid (TFA) in water (A), 0.1 % Trifluoroacetic acid (TFA) in acetonitrile (B); gradient: 5 % to 32 % of B within 40 min followed by 100 % of B in 44 min]. The product was eluted at R_t = 30.6 min (yield = 77 %). The HPLC chromatogram is shown in the **Fig. S37.** The product fraction was lyophilized and characterized by HRMS. HRMS (ESI-MS): calculated 962.8779 $[M+2H]^{2+}$, found 962.8755 $[M+2H]^{2+}$.

Synthesis of 3c (AZ647)

Compound **2c (AZ647)** (45 µg, 0.02 µmol) was dissolved in 20 µl dry DMF in a microcentrifuge tube, and to that, triethylamine (40.5 µg, 0.4 µmol) was added and the reaction mixture was stirred for 10 min at room temperature. After that, N, N'-Disuccinimidyl carbonate (102.47 µg, 0.4 µmol) was added and the reaction was allowed to continue overnight at room temperature. The crude product was purified using reverse-phase HPLC by using a 1 ml/min flow rate throughout the run [Solvent: 0.1 % Trifluoroacetic acid (TFA) in water (A), 0.1% Trifluoroacetic acid (TFA) in acetonitrile (B); gradient: 5 % to 32 % of B within 40 min followed by 100 % of B in 44 min]. The product was eluted at R_t = 31.2 min (yield = 94 %). The HPLC chromatogram is shown in the **Fig. S38.** The product fraction was lyophilized and characterized by HRMS. HRMS (ESI-MS): calculated 1011.3861 $[M+2H]^{2+}$, found 1011.3826 $[M+2H]^{2+}$.

General strategy for antibody conjugation: construction of CLEAR 488, CLEAR 568 and CLEAR 647 probes

a. In a typical conjugation experiment ~10 µg of primary antibody and ~60 µg of secondary antibody was used. The antibodies were buffer exchanged using Zeba™ spin desalting columns (7K MWCO) pre-equilibrated with 0.1M $NaHCO_3$ in PBS.
b. The antibodies were then allowed to react with 5 molar equivalents of the NHS ester derivatives of the photocleavable probes (**3a (AZ488)/ 3b (AZ568)/ 3c(AZ647)**). The reaction mixtures were kept at room temperature for 2 h and then further incubated overnight at 4°C to yield the CLEAR probes of different spectral regions.
c. The CLEAR probes were later purified using 7K MWCO Zeba™ spin desalting column pre-equilibrated with PBS.

d. After purification, concentrations of those **CLEAR 488, CLEAR 568 and CLEAR 647** probes were measured and stored at 4°C till their usage.

The typical conjugation efficiency was evaluated by determining the degree of labelling (DOL) from *UV–Vis* absorption spectra of the antibody conjugates. Using five equivalents of NHS ester derivatives of the corresponding photocleavable linker–fluorophore conjugates (fluorophores = AZ488, AZ568, or AZ647), a DOL in the range of approximately 1.4–2.7 fluorophores per antibody was obtained (see Supplementary Table 5). Importantly, this DOL range is comparable to that obtained when standard dye–NHS esters were directly conjugated to the same set of antibodies (see Supplementary Table 5 below), indicating that incorporation of the photocleavable linker does not compromise conjugation efficiency. Moreover, this range of labelling is optimal for fluorescence imaging, as higher labelling densities are known to induce self-quenching and can negatively affect antibody performance and signal brightness. These results therefore demonstrate that antibody conjugation via the photocleavable linker proceeds with high efficiency and is well suited for reproducible preparation and straightforward scaling.

***Supplementary Table 5**. Degree of labelling (DOL) of CLEAR antibody conjugates prepared via NHS ester conjugation.†*

Antibody conjugates	DOL
Donkey anti-rat-CLEAR-647	1.78
Donkey anti-rabbit-CLEAR-568	1.41
Donkey anti-rabbit-CLEAR-647	1.96
Donkey anti-human-CLEAR-488	2.7
Donkey anti-rabbit-CLEAR-488	2.27
Donkey anti-rat-AZ568	2.52

†*Degree of labelling (DOL) values determined from UV–Vis absorption spectra for CLEAR-based antibody conjugates synthesized using five molar equivalents of NHS ester–functionalized photocleavable linker–fluorophore conjugates (AZ488, AZ568, or AZ647). The table also includes a reference antibody conjugate prepared using a*

conventional fluorophore–NHS ester (AZ568) under identical reaction conditions for comparison. Comparable DOL values demonstrate that incorporation of the photocleavable linker does not compromise conjugation efficiency and supports reproducible preparation and scalability of CLEAR probes.

Construction of phalloidin-CLEAR-488 probe

Phalloidin amine (40.97 µg, 40.97 µl from a 1mg/ml stock in dry DMF, 0.05 µmol) was taken in a microcentrifuge tube and triethylamine (16.25 µg, 0.16 µmol) was added to that. The reaction mixture was stirred at room temperature for 10 min. After that **3a (AZ488)** (35 µg, 0.02 µmol) was added to the reaction mixture, and the reaction was allowed to proceed for another 3 h. The crude product was purified using reverse-phase analytical HPLC. The flow was kept at 1 ml/min, and the gradient was set as follows: The solvent mixture attains 5 % to 20 % of B in 8 min, 45 % of B in 30 min, followed by 100 % of B in 33 min. The product was eluted at 16.8 min (Yield: 78%). The HPLC chromatogram is shown in the **Fig. S30.** After purification, the product fraction was lyophilized and characterized by HRMS. HRMS (ESI-MS): Calculated, 1178.9430 $[M+2H]^{2+}$; found, 1178.9372, $[M+2H]^{2+}$.

C. Analysis of Photocleavage Products and Possible Byproducts from CLEAR-Based Probes, and Evaluation of Probe Stability under Storage Conditions

1. *UV-Vis* spectroscopy study of the photocleavable group

We examined the intrinsic photochemical reaction pathway of the photocleavable group, both in isolation and in the presence of biological complexity, in order to establish the primary reaction pathway and to evaluate whether secondary photoreactions or competing degradation processes occur upon irradiation in a biological environment. This was evaluated using *UV–Vis* spectroscopy. For this purpose, we used the compound **1d**, in which the photocleavable moiety serves as the primary chromophore unit. This compound contains the identical photocleavable group incorporated in the CLEAR probes and is synthesized as an intermediate during probe preparation. For the *UV–Vis* spectroscopy study, a 100 µM solution of the compound in PBS (200 µL) was prepared and placed in a quartz cuvette for measurement. The compound was then irradiated with a 365 nm LED light (47.19 mW/cm^2) in 15 s intervals, and *UV–Vis* absorption spectra were recorded after each irradiation step, with the total irradiation time reaching 120 s. The spectral evolution showed well-defined isosbestic points throughout irradiation (Fig. S1A and S1B), indicating a direct conversion between two dominant absorbing species (*I* and *II* in Fig. S1A) and supporting a single-step cleavage process. This observation confirms that the reaction proceeds through a clean bond-cleavage pathway, generating the expected photocleavage products (as illustrated in Fig. S1A and S1B) without detectable accumulation of intermediate species or secondary photoproducts. To assess whether biological complexity influences

the reaction pathway, the same compound **1d** was irradiated in the presence of 10 µg of cell lysate (HeLa) and analysed by *UV–Vis* spectroscopy. The spectral behaviour remained unchanged (Fig. S1C), with preserved isosbestic points, indicating that the photocleavage mechanism is maintained even in complex biological environments and proceeds without detectable side photoreactions.

2. Protocol for Matrix-Assisted Laser Desorption/Ionization Mass Spectrometry (MALDI-MS) analysis of cleaved photoproduct

Acetylated tubulin-CLEAR-647 antibody solution (2.5 µl in PBS) was irradiated with the 365 nm light for 120 seconds with a power density of 47.19 mW/cm^2. After that, the antibody solution was transferred to a microcentrifuge tube containing 2.5 µl of α-Cyano-4-hydroxycinnamic acid (CHCA) (saturated solution in 50:50 water (0.1% TFA)/acetonitrile) and was thoroughly mixed. The mixed solution was then placed onto a MALDI plate and allowed to dry at room temperature for analysis. After drying, the MALDI-MS analysis was performed and the raw data was extracted, plotted in GraphPad Prism 7 software package. As shown in Fig. S2, a mass signature corresponding to the cleaved fluorophore fragment was observed, consistent with the expected photocleavage product and supporting a similar single-step bond-cleavage mechanism in the conjugated CLEAR system.

3. Protocol for measuring the extent of hydrolysis in CLEAR probes

The stability of CLEAR conjugates during storage and under buffer conditions is a key parameter for their reproducible use and adaptation in multiplex imaging applications. To directly assess long-term stability, we re-examined the CLEAR probes that were synthesized approximately 3 years (2 years 9 months to 3 years 3 months) ago (Fig S8A). We evaluated the number of fluorophores that remained attached after this extended aging period. For this purpose, five different CLEAR conjugates (all 2 years 9 months to 3 years 3 months old) were passed through 7K Zeba™ spin desalting columns to separate any cleaved free fluorophore from the CLEAR antibody conjugates. Following column separation, the average number of fluorophores attached per antibody (i.e., the degree of labeling, DOL) was determined from *UV–Vis* absorption spectra and compared with the original DOL values of the CLEAR probes. We found that all CLEAR conjugates retained more than 80% of the originally attached fluorophores (typically 80–95%), even after approximately three years of storage in PBS at 4 °C. This observation indicates that CLEAR probes are only minimally affected by dark hydrolysis or spontaneous cleavage during storage (see more details in Fig. S8D).

D. Protocol for measurement of fluorescence lifetime

Time-resolved decay experiments were recorded on FLS1000 (Edinburgh instruments) for the conjugates of **AZ488** and **AZ568**, whereas a Horiba Delta Flex time-correlated single-photon-counting (TCSPC) instrument was used for the **AZ647** conjugates. Lifetime data of commercial dye NHS (**AZ488-NHS**, **AZ568-NHS** and **AZ647-NHS**) were used to compare with that of the respective photocleavable conjugates (**2a** (**AZ488**), **2b** (**AZ568**), **2c** (**AZ647**)). For the **AZ488** conjugates, excitation was carried out with 475 nm pulsed LASER and its emission was recorded at 517 nm, whereas for **AZ568** conjugates, the excitation wavelength was 510 nm, and its emission was recorded at 603 nm. For the case of **AZ647** conjugates, the excitation was carried out with 635 nm, and its emission was collected at 671 nm. The instrument response function (IRF) was collected by using a scatterer (Ludox AS40 colloidal silica). For each conjugate and the commercial dye, all the experiments were carried out at 200 nM concentration in PBS buffer (pH, 7.4). The lifetime data is shown in **Fig. S3**.

E. Protocols for the cellular imaging experiments

1. General Cell culture protocol:

a) A431, HeLa, U2OS, BS-C-1 and Jurkat cells were used for the experimental study.

b) A431 and HeLa cells were cultured in a humidified atmosphere (5 % CO_2) at 37°C and grown in Dulbecco's Modified Eagle's Medium (DMEM, high glucose) supplemented with 10 % fetal bovine serum (FBS) (Gibco, USA), 2 mM Glutamax (Invitrogen, USA) and 1 % antibiotics (100 U/ml penicillin, 100 µg/ml streptomycin and 0.25 µg/ml amphotericin) (Gibco, USA). U2OS cells were cultured in humidified atmosphere (5 % CO_2) at 37°C and grown in McCoy's 5A (Modified) Medium containing (+) L-Glutamine, supplemented with 10 % fetal bovine serum (FBS) (Gibco, USA), 2 mM Glutamax (Invitrogen, USA) and 1 % antibiotics (100 U/ml penicillin, 100 µg/ml streptomycin and 0.25 µg/ml amphotericin) (Gibco, USA). BS-C-1 cells were cultured in humidified atmosphere (5 % CO2) at 37°C and grown in Minimum Essential Medium (MEM) containing (+) non-essential amino acids (NEAA) and no glutamine, which was further supplemented with 10 % fetal bovine serum (FBS) (Gibco, USA), 2 mM Glutamax (Invitrogen, USA) and 1 % antibiotics (100U/ml penicillin, 100 µg/ml streptomycin and 0.25 µg/ml amphotericin) (Gibco, USA), 1 mM Sodium Pyruvate (Gibco, USA). Jurkat cells were cultured in RPMI media supplemented with the same percentages of FBS and antibiotics and 2 mM Glutamax (Invitrogen, USA).

c) At ~80% confluence, the cells were washed with DPBS (pH 7.3) (Gibco, USA), trypsinized, and suspended in a culture medium.
d) Cells were then counted, and in a typical experiment, 200 µL of cell suspension having ~10,000 cells/well were plated in an 8-well chamber slide system (Eppendorf, 1.5 glass bottom). Apart from the 8-well chamber, 35mm round imaging dishes (1.5 mm glass bottom) were also used for the imaging studies.
e) The cells were then again maintained in a humidified atmosphere (37°C, 5 % CO_2) for 24 h to reach ~ 60-80 % confluency.
f) Cells were subsequently used for imaging studies either in live conditions or after fixation, depending on the requirements of the experiment.

2. Determining fluorophore scission efficiency

2.1 Protocol for fluorophore scission experiment

U2OS cells were pre-extracted with 0.3 % Glutaraldehyde + 0.25 % Triton X-100 for 90 s and then fixed with 3% Glutaraldehyde for 10 min. Afterward, cells were rinsed twice with PBS and free aldehyde groups were reduced with 1mg/ml $NaBH_4$ in PBS for 5 min. After that, the cells were washed three times with PBS. Then the cells were permeabilized and blocked with 3 % BSA + 0.25 % Triton X-100 solution overnight at 4°C, and then subsequently washed with PBS prior to immunostaining. For imaging of microtubules, cells were first immunostained with α-tubulin primary antibody at 5 µg/ml concentration (diluted in 3 % BSA + 0.1 % Triton X-100 solution in PBS) for 1 h at room temperature and were subsequently washed three times with PBS (2 min incubation each). **CLEAR-647** secondary antibody probe was then incubated for another 1 h at a concentration of 5 µg/ml while keeping the sample at room temperature. After the incubation period was over, the sample was washed three times with PBS and mounted on the microscope. These LASER widefield images were acquired in Zeiss ELYRA PS1 inverted microscope using an oil immersion objective (alpha plan-Apochromat DIC 63x/1.40 oil DIC M27, NA = 1.40). After acquiring the first image, the sample was irradiated with a handheld 365 nm lamp (47.19 mW/cm^2) for 30 s, keeping the position fixed, and then reimaged. This cycle was repeated for up to 2 min of irradiation time while maintaining the same field of view. Microtubule filaments from different regions were taken for intensity measurement using Fiji ImageJ, and their respective background-corrected fluorescence intensity maxima (normalized) were plotted against the irradiation time to generate the decaying intensity curve. For the signal clearance experiment in mitochondria, 3 % glutaraldehyde fixed U2OS and BS-C-1 cells were used for **CLEAR-**

488 and **CLEAR-568** secondary antibody probes, respectively. The cells were permeabilized and blocked with a solution containing 3 % BSA + 0.25 % Triton X-100. The antibodies that were used for staining purposes include 5 µg/ml of TOM-20 primary antibody (species: mouse + rabbit) and 5 µg/ml of **CLEAR-488** (donkey anti-mouse) and **CLEAR-568** secondary antibody probe (donkey anti-rabbit). Each antibody was incubated for 1 h at room temperature. Prior to imaging, the excess secondary antibodies were removed by washing with PBS. Imaging was done using the same microscope setup as that of the microtubule experiment. Fluorescence intensity *vs* irradiation time was plotted by taking into account the background-corrected intensity maxima (normalized) of several mitochondrial regions. The normalization was performed by using Microsoft Excel and then plotted using the GraphPad Prism 7 software package. For the EGFR target, 4 % PFA fixed A431 cells were stained with Cetuximab (5 µg/ml) for 1 h at room temperature, followed by washing with PBS and incubation with the respective **CLEAR-488** secondary antibody probe (5 µg/ml) for another 1 h at room temperature. Subsequently, the EGFR was imaged by using the same imaging and erasing protocol followed for the microtubules. Three LASERs were used at 1 % power for all (488 nm, 561 nm, 642 nm) microtubule-related widefield imaging. For mitochondria, 488 nm (0.5 %) and 561 nm LASER (1 %) were used, whereas for EGFR, 488 nm LASER was used (0.6 %).

2.2 Fluorophore scission over a large area

For the large area imaging, U2OS cells were seeded in a 35 mm dish, and after 24 h of cell seeding, U2OS cells were pre-extracted with 0.3 % Glutaraldehyde + 0.25 % Triton X-100 for 90 sec and then fixed with 3 % Glutaraldehyde for 10 min. Afterward, cells were rinsed twice with PBS, and free aldehyde groups were reduced with 1 mg/ml $NaBH_4$ in PBS for 5 min. After that, the cells were washed three times with PBS, and then the cells were permeabilized and blocked with 3 % BSA + 0.25 % Triton X-100 overnight at 4°C. The cells were stained with the α-tubulin primary antibody (5 µg/ml) for 1 h, followed by washing with PBS and then incubated with the respective **CLEAR-488** secondary antibody probe (5 µg/ml) at room temperature for 1 h. In the microscope, a cellular area of ~ 1.02 mm ×1.00 mm was scanned before and after the irradiation (2 min of irradiation with a 365 nm lamp with a power density of 64.20 mW/cm^2). This imaging experiment was performed in a Leica TCS SP8 confocal microscope with a 488 nm LASER (Source: 20 mW) at 0.18 % power (Emission collection, 510-600 nm). The images acquired were processed using LAS X and ImageJ software.

3. Protocol for assessing the role of photobleaching in signal reduction

In an 8-well LabTek chamber, U2OS cells were pre-extracted with 0.3 % Glutaraldehyde + 0.25 % Triton X-100 for 90 sec and then fixed with 3% Glutaraldehyde for 10 min. Afterward, cells were rinsed twice with PBS and free aldehyde groups were reduced with 1 mg/ml $NaBH_4$ in PBS for 5 min, followed by three times washing with PBS. Then the cells were permeabilized and blocked for 12 h at 4°C using 3 % BSA + 0.25 % Triton X-100 solution. In three separate wells, cells were stained with α-tubulin primary antibody (5 µg/ml) for 1 h at room temperature, which was followed by washing with PBS and incubation with donkey anti-rat-488/568/647 secondary antibodies (control antibodies where fluorophores are attached without a photocleavable linker) for 1 h at room temperature. Imaging was performed in a Zeiss ELYRA PS1 inverted microscope using an oil immersion objective (alpha plan-Apochromat DIC 63x/1.40 oil DIC M27, NA = 1.40). At first, a region was fixed where bright microtubule signals were visible, and an image was acquired from that region. This was followed by irradiation of the sample for 2 min with the 365 nm lamp (47.19 mW/cm^2) and reimaging the same region with the same microscope setting used for acquiring the image before 365 nm irradiation. This set of steps was followed for all three cases of the fluorophores. Upon acquiring the images (**Fig. S4A**). before and after 365 nm, mean intensities from three different square regions were picked up from the two images, normalized, and plotted using GraphPad Prism 7 software package (**Fig. S4B**). For this same study on the EGFR membrane, A431 cells were fixed with 4 % PFA in a 35 mm imaging dish and followed by a blocking step with 3 % BSA solution in PBS. EGFR was stained with Cetuximab (5 µg/ml) for 1 h at room temperature. This was followed by washing with PBS and incubation with donkey anti-human-488 secondary antibody (5 µg/ml, control antibodies where fluorophores are attached without a photocleavable linker) for another 1 h, and then imaged under the same microscopic settings used for its **CLEAR-488** counterpart to image EGFR. In short, EGFR was imaged in a cellular region and then irradiated with a 365 nm lamp for 30 s, and the same region was reimaged. This process was repeated up to 120 s irradiation time, and a line profile was drawn over a membrane area on the images corresponding to 0 s of 365 nm irradiation and 120 s of 365 nm irradiation (**Fig. S5A**). Intensity values were extracted and plotted using the GraphPad Prism 7 software package for comparison (**Fig. S5B**).

4. Protocol for antigenicity retention experiment

In an 8-well LabTek chamber, U2OS cells were pre-extracted with 0.3 % Glutaraldehyde + 0.25 % Triton X-100 for 90 sec and then fixed with 3 % Glutaraldehyde for 10 min. Afterward, cells were rinsed twice with PBS and free aldehyde groups were reduced with 1 mg/ml $NaBH_4$ in PBS for 5 min. After that, three times washing with PBS was performed on the cells and, then permeabilized and

blocked for 12 h at 4°C using 3 % BSA + 0.25 % Triton X-100 solution. For the control sample, the blocking solution was removed prior to immunostaining and then the α-tubulin primary antibody (5 µg/ml) was incubated for 1 h at room temperature. After the incubation period, the unbound primary antibody was removed, and the sample was washed three times (with 5 min incubation) with PBS. Later, the respective **CLEAR-488** secondary antibody probe (5 µg/ml) was incubated for another 1 h. After this incubation period, the cells were washed three times with PBS and then mounted over the microscope for imaging. Confocal microscopy was performed with 488 nm LASER (Emission collected, 510-600 nm). For comparison with an irradiated sample, in a separate well, the cells were irradiated with a 365 nm (47.19 mW/cm^2) lamp for a total of 20 irradiation cycles, with each cycle consisting of 1 minute of illumination, corresponding to a total irradiation time of 20 minutes. After the irradiation step, the cells were immunostained with α-tubulin primary antibody (5 µg/ml) followed by **CLEAR-488** secondary antibody probe (5 µg/ml) by maintaining the same conditions as those of the control sample. Then the cells were imaged applying the same microscope parameters as those of the control sample. For comparison, three images for both conditions were taken, and from there, ten square regions having well-spread microtubules and similar microtubule density were considered for intensity measurement (**Fig. S6**). The intensity values were plotted as a bar diagram with an error bar using GraphPad Prism 7 software.

5. Imaging protocol for cycling experiment

5.1 Single fluorophore in each round of imaging

A431 cells were cultured in a 35 mm imaging dish for 24 h and then fixed with 4 % PFA in PBS for 15 min. Afterward, cells were rinsed twice with PBS and free aldehyde groups were reduced with 1 mg/ml $NaBH_4$ in PBS for 5 min, followed by three times washing with PBS. Cells were then permeabilized and blocked with blocking buffer (3 % BSA + 0.25 % Triton X-100) overnight at 4°C. After that, the cells were stained with the respective primary antibodies of mitochondria, Cytokeratin 18, α-tubulin, and EGFR at a 5 µg/ml concentration for 45 min. In parallel, the nucleus was stained with Hoechst 33342 at a concentration of 1 µg/ml. After this incubation period, quick washes (three times) with PBS was performed and, the respective **CLEAR-488** secondary antibody probe against mitochondria (10 µg/ml) was incubated for another 45 min and then washed three times with PBS and imaged. The confocal microscopy was performed with a 488 nm LASER using an oil immersion objective (HC PL APO 63x/1.40 OIL CS2). After imaging each target, 365 nm light (64.2 mW/cm^2) irradiation was performed for two min, and then the sample was washed twice with PBS to remove the cleaved fluorophores. This process was repeated for Cytokeratin 18, α-tubulin, and EGFR with their

respective **CLEAR-488** secondary antibodies. After imaging EGFR and erasing its signal from the membrane, **phalloidin-CLEAR-488** (5 µM in PBS) was incubated for 1 h at room temperature to stain actin filaments. After 1 h, the unbound phalloidin molecules were washed out, and actin filaments were imaged. This was followed by the final round of imaging, where glycolipids and glycoproteins were stained with WGA-FITC label (5 µg/ml). The LASER (488 nm) power was varied for each target to have a sufficient signal. For each target, imaging was performed in different z-planes (~16-19 stacks for each target) with varying separations between stacks to make sure all the targets were acquired from the best image planes possible. The same field of view was maintained throughout the whole experiment. The images acquired were processed using LAS X and ImageJ software. The imaging parameters are given in **Supplementary Table 6**.

Supplementary Table 6: *LASER power and the stack details for the cycling experiment*

Target	**LASER (488nm) power**	**Total stacks**	**Stack separation (µm)**
Mitochondria	0.5 %	16	1
Cytokeratin 18	0.5 %	19	1
EGFR	0.25 %	16	0.7
α-tubulin	0.5 %	16	0.35
Actin	0.15 %	17	0.12
Glycolipids and glycoproteins	0.35 %	16	0.6

5.2 Three fluorophores in each round of imaging

A431 cells were cultured and seeded in a 35 mm imaging dish. After 24 h, the cells were fixed with 4 % PFA for 15 min Afterward, the cells were rinsed twice with PBS, and free aldehyde groups were reduced with 1 mg/ml $NaBH_4$ in PBS for 5 min, followed by three times washing with PBS. Then the cells were blocked and permeabilized for overnight at 4°C with 3 % BSA + 0.25 % Triton X-100. For the first round of the three-color imaging cycle, cytokeratin 18 (final concentration of 5µg/ml) and TOM20 (final concentration of 5 µg/ml) primary antibodies were mixed in antibody dilution buffer (3 % BSA + 0.1 % Triton X-100) and incubated for a duration of 45 min at room temperature. Upon finishing the incubation period, cells were washed with PBS (3 times) and a cocktail solution containing the respective **CLEAR-568** secondary antibody probe (10 µg/ml) for cytokeratin 18, **CLEAR-647** secondary antibody probe (10 µg/ml) for TOM20, Hoechst 33342 (1 µg/ml) and

Phalloidin-CLEAR-488 (final concentration of 5 µM) were incubated for 45 min at room temperature and then washed three times with PBS. The imaging dish was then mounted over the microscope, and the targets were imaged in four different channels (405 nm, 488 nm, 552 nm, 638 nm) over multiple z-planes. After the first imaging round, fluorophores were cleaved using a 365 nm LED lamp (64.2 mW/cm^2) for 2 min and then the cells were washed with PBS (2 times) to remove the cleaved fluorophores from the solution. The second round of immunostaining involved α-tubulin (5 µg/ml), and cetuximab EGFR (5 µg/ml) primary antibody incubation for 45 min at room temperature, followed by 2-3 times washing with PBS and then incubation of the cocktail solution containing WGA-FITC stain (5 µg/ml), **CLEAR-568** secondary antibody probe (10 µg/ml) for EGFR & **CLEAR-647** antibody probe for α-tubulin (10 µg/ml) for a duration of 45 min at room temperature. Once the incubation period was over, cells were washed with PBS (three times) and then imaged again in the same field of view. The images were acquired in a Leica TCS SP8 confocal microscope using an oil immersion objective (HC PL APO 63x/1,40 OIL CS2). The images acquired were processed using LAS X and ImageJ software. The imaging details are given in **Supplementary Table 7**.

Supplementary Table 7: *LASER power and the antibodies used for the multiplexed cellular imaging in fixed A431 cells*

Cycles	Target	LASER (% Power)	Primary staining	2°Ab	Fluorophore
1st	Nucleus	405 nm (0.15 %)	-	-	Hoechst33342
	Actin	488 nm (0.1 %)	Phalloidin-CLEAR-488	-	AZDye488
	Cytokeratin 18	552 nm (0.25 %)	anti-Cytokeratin 18	CLEAR-568 (donkey anti-Rabbit)	AZDye568
	Mitochondria	638 nm (4.5 %)	anti-TOM20	CLEAR-647 (donkey anti-Mouse)	AZDye647
2nd	Nucleus	405 nm (0.15 %)	-	-	Hoechst33342
	Glycolipids and glycoproteins	488 nm (0.15 %)	WGA	-	FITC
	EGFR	552 nm (0.25 %)	Cetuximab	CLEAR-568 (donkey anti-Human)	AZDye568

	α-tubulin	638 nm (0.4 %)	anti-α-tubulin	CLEAR-647 (donkey anti-Rat)	AZDye647

5.3 Imaging performance of the aged CLEAR probes.

The stability of CLEAR conjugates during storage and under buffer conditions is a key parameter for their reproducible use and adaptation in multiplex imaging applications. To directly assess long-term stability, we examined the imaging performance of CLEAR probes that were synthesized approximately 3 years (2 years 9 months to 3 years 3 months) ago. These were stored in phosphate-buffered saline (PBS) at 4 °C, wrapped in aluminum foil to prevent light exposure, and intermittently reused under typical laboratory handling conditions (Fig. S8A). As shown below in Fig. S8B & S8C, these aged CLEAR probes remained functionally intact, retaining both their imaging capability and light-triggered signal erasure behavior. Experimentally, the retained stability was validated by staining TOM20 and α-tubulin using aged AZ488- and AZ647-based CLEAR probes, respectively, followed by visualization using confocal microscopy. In both cases (see Fig. S8B), the aged CLEAR probes enabled high-contrast and specific visualization of mitochondrial structures (TOM20 staining) and microtubule structures (α-tubulin staining). These results indicate that prolonged storage does not lead to a noticeable loss of probe integrity or imaging performance. To further examine the chemical integrity of the photocleavable linker, we evaluated whether long-term storage affected photocleavage efficiency. Upon irradiation, the fluorescence signal was efficiently erased within approximately 120 s (Fig. S8C). The preservation of rapid and efficient signal removal indicates that the linker remains largely intact during storage and under buffer conditions and does not undergo appreciable spontaneous cleavage or hydrolysis over time. This functional assay provides consistent evidence that CLEAR conjugates exhibit good long-term stability under standard buffer and storage conditions, making them suitable for reproducible use and adaptation in multiplex imaging applications.

6. Imaging protocol for high-dimensional imaging of Jurkat cells undergoing immunological synapse formation

An 8-well coverslip-bottomed chamber was coated with a solution of 2 µg/mL anti-human CD3 and 1 µg/mL His-ICAM overnight, at 37°C. Just prior to cell addition, wells were washed twice with PBS. 0.1 million Jurkat cells (immortalized human T lymphocyte cell line) were suspended in complete RPMI media (with 10 % FBS, 1X Pen-Strep, 50 µM beta-mercaptoethanol, and 100 µM Sodium

pyruvate) and were added to each well and allowed to form immunological synapses at 37°C for 5 min. Two rounds of PBS washes to remove unbound cells were followed immediately by fixation for 20 min at room temperature with 3.7 % PFA in 1X PHEM buffer (18.14 g PIPES, 6.5 g HEPES, 3.8 g EGTA, 0.99 g MgSO4, pH 7.0 adjusted with KOH in 1 L water), then permeabilization with 0.1 % Triton X-100. This was followed by two brief PBS washes. The cells were then incubated with 5 µg/ml p-ZAP70, NUP98, and TOM20 primary antibodies diluted in 3 % BSA + 0.1 % Triton X-100 for 45 min at room temperature. This was followed by three brief washes with PBS and then the incubation of CLEAR probes against the incubated primary antibodies (**CLEAR-488** secondary antibody probe against p-ZAP70, **CLEAR-568** against NUP98, and **CLEAR-647** against TOM20 at a concentration of 5 µg/ml) for another 45 min at room temperature. When the incubation period was over, the cells were washed three times with PBS and imaged. Once the imaging of all three targets was performed, the cells were irradiated with the 365 nm lamp for 2 min (47.19 mW/cm^2) and then washed three times with PBS. The second round of staining was performed with the **clathrin-CLEAR-488** primary antibody probe (10 µg/ml), **α-tubulin-CLEAR-568** primary antibody probe (10 µg/ml), and **acetylated tubulin-CLEAR-647** (10 µg/ml) primary antibody probe for 45 min at room temperature. This labelling period was followed by three brief washes with PBS and imaging. The three targets were imaged in different z-planes, and after the image acquisition, the cells were again irradiated with a 365 nm lamp to erase the signals from these targets. In the 3rd round of labelling, actin was stained with a 2 µM solution of **phalloidin-CLEAR-488** in PBS for 45 min at room temperature. It was followed by three brief washes with PBS to remove the unbound phalloidin molecules and imaging the actins. Eventually, the sample was irradiated with the 365 nm lamp after imaging the actin to cleave the fluorophores from the phalloidin molecules. In the last round of imaging, cells were first stained with WGA-FITC (5 µg/ml), paxillin (5 µg/ml), and lamin B1- CLEAR-647 primary antibody probe (10 µg/ml) for 45 min at room temperature. Later, the cells were washed with PBS and then incubated with CLEAR-568 secondary antibody probe against paxillin (5 µg/ml). The cells were then given three brief washes after 45 min and imaged in different z-planes. The images were acquired in a Leica TCS SP8 confocal microscope using an oil immersion objective (HC PL APO 63x/1,40 OIL CS2). The images acquired were processed using LASX and ImageJ software. The imaging details are given in Supplementary Table 8.

Supplementary Table 8: *LASER power and the antibodies used for the multiplexed cellular imaging in fixed Jurkat cells.*

Cycles	Target	LASER (%	1°Ab	2°Ab	Fluorophor

		Power)			e
1st	p-ZAP70	488 nm (1 %)	p-ZAP70	**CLEAR-488** (donkey anti rabbit)	AZDye488
	NUP98	552 nm (1.8 %)	NUP98	**CLEAR-568** (donkey anti-Rat)	AZDye568
	Mitochondria	638 nm (1.5 %)	TOM20	**CLEAR-647** (donkey anti-Mouse)	AZDye647
2nd	Clathrin	488 nm (1 %)	**Clathrin-CLEAR-488**	-	AZDye488
	α-tubulin	552 nm (1.8 %)	**α-tubulin-CLEAR-568**	-	AZDye568
	Ac-tubulin	638 nm (1.5 %)	**Ac-tubulin-CLEAR-647**	-	AZDye647
3rd	Actin	488 nm (0.1 %)	**Phalloidin-CLEAR-488**	-	AZDye488
4th	Glycoprotein & Glycolipids	488 nm (1 %)	WGA-FITC	-	FITC
	Paxillin	552 nm (1.8 %)	Paxillin	**CLEAR-568** (Donkey anti sheep)	AZDye568
	Lamin B1	638 nm (1.5 %)	**Lamin B1-CLEAR-647**	-	AZDye647

F. Protocol for multiplexed tissue imaging using CLEAR probes

1. Drosophila ovary tissue section

For dissecting ovary tissues, female adult flies were taken and submerged in PBS. The fly was grabbed at lower part of its thorax with a forcep and was gently tugged at the lower thoracic abdomen with another forcep until the internal organs in the abdomen were exposed. On identifying the ovary pair, they were detached from other organs and transferred to chilled PBS in a dish. After the dissection of sufficient sample, tissues were fixed with 4 % paraformaldehyde (PFA) at room temperature for 30 min with gentle shaking. Then, the fixed tissues were washed at least three times for 5 min each with PBS + 0.5 % Triton X-100 (0.5 % PBT), followed by blocking the samples for 1 h at room temperature with 10 % horse serum in 0.5 % PBT. Upon finishing the blocking period, the tissue sample was first

stained with anti-α tubulin primary antibody at a 10 µg/ml concentration for 1 h at room temperature. This was followed by gentle washing with PBT buffer (PBS + 0.5 % Triton X-100) and secondary immunostaining for another 1 h with **CLEAR-647** secondary antibody probe (10 µg/ml). Hoechst 33342 (10 µg/ml) was used for nuclear staining. The tissue sample was washed with PBT to remove excess antibodies and then taken for confocal imaging. The confocal imaging of the tissue was performed using an oil immersion objective (HC PL APO 63x/1,40 OIL CS2) by exciting the fluorophore with 2 % power of 638 nm diode LASER (Emission collection, 660 nm-750 nm). Hoechst excitation was performed using a 405 nm diode LASER (Emission collection, 425nm - 550 nm). After the first round of imaging, the tissue sample was irradiated with a 365 nm (120.93 mW/cm^2) lamp for 2 min and then washed gently with 0.5 % PBT. The second round of staining involved **Phalloidin-CLEAR-488** (5 µM) incubation for 1 h at room temperature and then subsequently imaging under the microscope after a gentle wash with 0.5 % PBT. 1 % power of 488 nm LASER was used for the excitation (Emission collection, 510 nm-600 nm) of the phalloidin probe. The images acquired were processed using LASX and ImageJ software.

2. Mouse lymph node tissue section

All animal experiments were performed in accordance with institutional guidelines and were approved (approval No. SA004) by the Institutional Animal Ethics Committee (IAEC) of JNCASR. After tissue dissection, the lymph node was put in 1x PBS and then fixed with 4 % PFA overnight at 4°C. After the fixation period was over, the sample was washed three times with 1x PBS (10 min for each wash). Then, the lymph node section was transferred to a 15 % sucrose solution prepared in autoclaved Milli-Q water and kept there overnight at 4°C. After this, the lymph node section was again transferred to a 30 % sucrose solution and kept overnight. After that, the lymph node sections were washed with PBS (3 times with a 10-minute duration) and stored by keeping them immersed in polyfreeze media at -80°C until further use. For use in an imaging experiment, the frozen lymph node was cryo-sectioned into slices of 50-100 µm thickness and placed in a gelatin-coated 35 mm imaging dish. The lymph node section was washed several times with PBS to remove the viscous polyfreeze media before immunostaining. Once the viscous media was removed from the imaging dish, the lymph node section was incubated with B220 primary antibody solution (10 µg/ml in 3 % BSA + 0.1 % Triton X-100 solution) overnight at 4°C. After that the section was gently washed three times with PBS to remove the unbound primary antibodies and then incubated with **CLEAR-647** secondary antibody probes against the B220 primary antibody (15 µg/ml in 3 % BSA + 0.1 % Triton X-100 solution) for another

4 h at room temperature. After that, the sample was washed three times again with PBS (5 min duration) and was taken for imaging. The imaging was performed using a confocal microscope by scanning several different tiles. The 638 nm LASER was used for the imaging. After the B220 target was imaged, the sample was irradiated with 365 nm lamp at a power density of 120.93 mW/cm^2 for 4 min and then washed with PBS three times (3 min duration) to remove the cleaved fluorophores from the solution. After these washing steps, the CD4-Alexa Fluor647 primary antibody was incubated for 4 h at room temperature (1:50 dilution). Then the sample was again washed three times with PBS to remove the unbound primary antibody. After this, the sample was imaged while maintaining the same region of interest. The image processing was done using LASX and the Fiji ImageJ software package.

G. Super-resolution dSTORM imaging using CLEAR probes

U2OS cells were cultured and plated in an 8-well LabTek chamber (10000-12000 cells per well) 24 h prior to imaging. The cells were fixed with 4 % PFA for 15 min. Afterward, cells were rinsed twice with PBS and free aldehyde groups were reduced with 1 mg/ml $NaBH_4$ in PBS for 5 min, followed by three times washing with PBS. Then the cells were permeabilized and blocked with 3 % BSA + 0.25 % Triton X-100 overnight at 4°C. For the first round of imaging, anti-TOM20 antibody (rabbit) (10 µg/ml) was incubated for 45 min at room temperature and then later washed three times (5 min) with PBS. After that, **CLEAR-647** secondary antibody probe (donkey anti-Rabbit,10 µg/ml) was incubated for another 45 min at room temperature. Upon finishing the incubation period, the excess secondary antibodies were removed by washing three times (10 min incubation time) with PBS. After this thorough washing, STORM imaging buffer, which consists of TN buffer (50 mM Tris (pH 8.0) + 10 mM NaCl + 10 % w/v glucose), an oxygen scavenging system (0.5 mg/ml glucose oxidase, 40 µg/ml catalase, and 100 mM MEA) was put in the imaging well and mounted for imaging. Images were acquired using a Zeiss Elyra PS1 inverted microscope with an oil immersion TIRF objective (alpha Plan-apochromat DIC 100 x /1.46 Oil DIC M27, NA = 1.46). A 642 nm diode LASER was used to excite the fluorophore. Fluorescence light was spectrally filtered with an emission filter (MBS-642 + EF LP 655) and imaged by an electron-multiplying charge-coupled device (EMCCD) camera (Andor iXon DU897, QY> 90 %, 512 × 512 pixels). After acquiring the image of the mitochondria, the imaging buffer was removed from the imaging well and the cells were washed with PBS (three times with 5 min incubation) and then irradiated with a 365 nm lamp (47.19 mW/cm^2) for two min and again washed three times with PBS to make sure the cleaved fluorophores were removed and do not contribute to non-specific signals. For the second round of imaging, an anti-vimentin primary antibody

(10 µg/ml) was incubated for 45 min. After that, the cells were washed three times (10 min) with PBS, and **CLEAR-647** secondary antibody probe (donkey anti-mouse) at 10 µg/ml concentration was incubated for 45 min at room temperature. After this incubation period, cells were washed three times (10 min) with PBS to remove excess secondary antibodies. Later, the imaging well was replenished with fresh STORM imaging buffer, and the vimentin filaments were imaged from the same field of view. Post-image acquisition, the washing and cleaving of fluorophores were repeated in the same way as in the first round. For the third round of imaging, anti-α-tubulin primary antibody (10 µg/ml) was incubated for 45 min, followed by washing three times with PBS, and then incubation of **CLEAR-647** secondary antibody probe (donkey anti-Rat) at 10 µg/ml concentration for 45 min. The incubation period was kept the same for both antibodies as that of the other two targets. After washing the excess secondary antibodies, the well was replenished with fresh STORM imaging buffer, and microtubules were imaged. For all three targets, a 642 nm diode LASER was used (0.9 kW-1.1 kW cm^2) with a frame rate of 50 Hz while maintaining the same field of view for all three targets, and 10000-12000 frames of images were acquired. The STORM images were processed in the Picasso software package and Fiji ImageJ.

H. Protocols for imaging experiments in live cells

1. Determination of fluorophore scission efficiency

A431 cells, cultured in a 35 mm imaging dish 24 h prior to imaging, were washed three times with DPBS to remove the media. Cells were immunostained with **anti-EGFR-CLEAR-488** (5 µg/ml) antibody for 10 min, followed by two quick washes (~5 s) with DPBS and finally restoring the cells in phenol red-free DMEM for imaging. Subsequently, the cells were imaged in a live cell-imaging setup in confocal microscope, and this was followed by 30 s of 365 nm (47.19 mW/cm^2) irradiation. This imaging and irradiation cycle was performed for three more rounds for a total irradiation time of 90 s. The EGFR signal was diminished significantly (> 99 %) within 90 s of irradiation with the 365 nm lamp. The images were acquired in a Leica TCS SP8 Confocal microscope using 488 nm LASER for the excitation (Emission collection, 510 – 600 nm). An oil immersion objective was used in the process (HC PL APO 63x/1.40 OIL CS2). The confocal images were processed in LASX and Fiji ImageJ software. Intensity values were extracted using ImageJ by drawing a line profile over a section of the membrane showing EGFR staining. The intensity values along the line were plotted against irradiation time. These values were normalized in Microsoft Excel and then plotted against irradiation time using GraphPad Prism 7 software.

2. Imaging a single target with two different fluorophores

To show the multiplexing ability in live cells, A431 cells were cultured in a 35 mm imaging dish for 24 h prior to the imaging. The media was removed, and the cells were briefly washed with DPBS (three times). First, the cells were stained with **anti-EGFR-CLEAR-488** antibody probe (2.5 µg/ml) for 10 min inside the live cell imaging setup (37°C, 5 % CO_2). Then the unbound antibodies were taken out by three quick washes (~5 s) using DPBS. After washing, the DPBS was replaced by phenol red-free media, and the cells were imaged with 488 nm LASER (1 %) in Leica SP8 confocal microscope using an air objective (HC PL APO CS2 20x/0.75). Emission from the fluorophore was collected in the window of 510-600 nm. After the first round of EGFR imaging, the cells were irradiated with the 365 nm (47.19 mW/cm^2) lamp for a total of 90 s in three rounds spanning 30 s each. The cells were washed twice with DPBS to remove the cleaved fluorophores. For the second cycle of imaging, unlabelled primary anti-EGFR antibody (2.5 µg/ml) was applied to the cells for 10 min followed by quick washing (5 s each) with DPBS and incubation of **CLEAR-647** (donkey anti-Human) at 2.5 µg/ml concentration for 10 min. After the incubation period, cells were washed three times with DPBS, and eventually, they were provided with fresh media for imaging. A 638 nm (Emission collected 660-750 nm) LASER (5 %) was used to excite the probe. After image acquisition in the red channel, the cells were irradiated with 365 nm (47.19 mW/cm^2) for 90 s. This irradiation was followed by Calcein AM staining (1 µM). All the cells reported their viability by showing bright Calcein AM staining. Some regions although displayed weak Calcein stating in Fig. 8C-VI, this was attributed to apparent inhomogeneity arises primarily from imaging-plane effects rather than from reduced probe performance or compromised cell viability. The experiments were performed using A431 cells, which are epithelial in nature and typically grow in dense, tightly packed colonies (clusters), resulting in uneven monolayers with variations in cell height and morphology. Consequently, during confocal imaging, only cells located within the focal plane display maximal cytosolic fluorescence, whereas cells positioned slightly above or below the focal plane appear dimmer due to reduced signal collection. In the image presented in Fig. 8C–VI, fluorescence from a single confocal plane is shown, and therefore, cells residing outside this focal plane appear weaker in intensity despite remaining viable and properly labeled.

To further validate this explanation, in the revised manuscript we re-examined irradiated A431 cells using three-dimensional (z-stack) imaging. In these additional live-cell experiments, cells were first irradiated with a 365 nm lamp for 180 s and subsequently stained with Calcein AM. Confocal images acquired from multiple z-planes within the same region of interest (see Fig. S19) clearly demonstrate that cells exhibiting weaker fluorescence in one imaging plane display strong cytosolic fluorescence when imaged at the appropriate focal depth. Importantly, when the full z-stack is considered, all cells within the imaged region exhibit bright cytosolic fluorescence, confirming that the observed intensity

variation arises from focal-plane differences rather than loss of viability or diminished staining efficiency. Furthermore, the uniform cytosolic conversion and retention of Calcein AM across irradiated cells indicate preserved membrane integrity and metabolic activity, demonstrating that the applied 365 nm light irradiation conditions do not adversely affect cell viability. These observations therefore indicate that the weak signal observed in certain regions originates from imaging-plane effects and not from compromised cell health, UV-induced damage, or reduced probe performance. The images were processed with LAS X and ImageJ software package.

I. Evaluation of cellular toxicity in combination of 365 nm light and photocleaved products

We evaluated whether the photocleavage products and the associated light exposure cycles exert any adverse effects on cellular health under imaging-relevant conditions. To address this, cell viability assays were performed in HeLa cells using four complementary experimental conditions designed to independently examine molecular-level photoproduct effects both in isolation and in antibody-coupled imaging configurations (Fig. S20). Two experimental sets employed small-molecule surrogate compounds that reproduce the chemical structure of the photocleavable linker (**1**) and the associated fluorophore conjugate (**2c**), enabling assessment of the intrinsic toxicity of the released photoproducts independent of antibody targeting or cellular localization. The remaining two conditions employed antibody-conjugated CLEAR probes to closely mimic realistic imaging scenarios involving receptor targeting and iterative signal-erasing steps. In the first two experimental sets, cells were incubated with the small-molecule surrogate compounds **1** and **2c** at concentrations corresponding to those expected for highly expressed receptors (EGFR was used as a representative example). This was followed by irradiation for 180 s, corresponding to two erasing cycles typically used in live-cell imaging experiments. This condition evaluates the direct effect of freely generated photocleavage products on cellular viability. In the third set, cells were treated with cetuximab followed by donkey anti-human CLEAR-488 and irradiated for 90 s to simulate a single erasing step under antibody-based imaging conditions. In the final set, sequential antibody labelling and two rounds of irradiation (90 s each) were performed to reproduce consecutive erasing cycles commonly used during multiplexed imaging experiments. Cell viability was quantified 24 h after irradiation to capture any immediate or delayed adverse effects on cellular health. As shown in Fig. S20, cell viability remained largely unaffected across all experimental conditions, indicating that neither the generated photocleavage products nor 365 nm light irradiation under the applied conditions induced measurable cytotoxic effects. The experimental details are described below:

HeLa cells were seeded at a density of 12,000 cells per well in 96-well plates and allowed to adhere and grow for 24 h under standard culture conditions. Prior to all treatments, cells were washed once with 1× phosphate-buffered saline (PBS). Following incubation with the specified compound, cells were subjected to 365 nm irradiation as described below. The cells were incubated with 10 fmol of compounds **1** and **2c** (prepared in 100 µl of complete cell culture medium as 0.1 nM solution) for 30 min. The corresponding amount was calculated based on the estimated number of EGFR receptors present per HeLa cell (*Anal. Chem.* 2015, **87**, 19, 9960–9965), such that the number of molecules of compounds **1d** and **2c** matched the total receptor count under the experimental conditions. Calculation for the number of molecules of 1d and 2c required is shown below. Subsequently, cells were exposed to one cycle of 365 nm light irradiation (90 s total exposure, applied as three pulses of 30 s each), followed by incubation for 1 h in an incubator. After that a second 365 nm light irradiation cycle (90 s total exposure, applied as three pulses of 30 s each), was then applied and again placed in the incubator. After 24 h, the cell viability was assessed by Alamar Blue assay. The toxicity profile is shown in Figure S20 (A-B).

Calculation of the number of molecules of 1d and 2c required to match the estimated number of EGFR receptors in HeLa cells:

Expression of EGFR per HeLa cell ~0.5 million (*Anal. Chem.* 2015, **87**, 19, 9960–9965)

Number of cells per well ~ 12000

Number of total EGFR in a well ~ 12000 × 500000

$$= 6.0 \times 10^{9}$$

Number of moles ~ $6.0 \times 10^{9} / (6.0223 \times 10^{23})$

$$= 1.0 \times 10^{-14}\ \text{mol}$$

$$= 10\ \text{fmol}$$

To evaluate cellular toxicity resulting from antibody incubation combined with 365 nm light exposure, HeLa cells were first incubated with Cetuximab primary antibody (5 µg/mL) for 15 min. Cells were then washed three times with 1× PBS and incubated with the corresponding secondary antibody, donkey anti-human-CLEAR-488 (5 µg/mL) for 15 min, followed by three additional PBS washes. After this antibody labeling step, cells were exposed to one cycle of 365 nm light irradiation (90 s total irradiation, applied as three pulses of 30 s each). One set of cells were kept in the incubator for 1 h after the 365 nm light irradiation which was followed by a second round of antibody labeling was

performed using a Trastuzumab primary antibody (5 µg/mL) and secondary antibody (donkey anti-human-CLEAR-488, 5 µg/mL), following the same incubation and washing protocol. After completion of this second antibody staining procedure, cells were subjected to an additional 365 nm light irradiation cycle (a total of 180 s) and were then placed in the incubator for 24 h. After 24 h, the cell viability status was assessed by Alamar Blue assay. The toxicity profile is shown in Figure S20 (C-D).

Once this 24 h incubation period was over, the cells were then washed with PBS three times, and 10 % Alamar Blue in complete culture medium was added to each well (100 µl) and further incubated at 37°C for 4 h. After 4 h, absorbance was measured at 570 nm (experimental wavelength) and 600 nm (reference wavelength) using a Plate Reader (Synergy H1, BioTek), and cellular viability was determined. GraphPad Prism 7 software was used to plot the data relevant to the cell viability status. Cellular viability was determined by using the formula shown below:

Percentage of cell viability (%) = $(O_2 \times A_1) - (O_1 \times A_2)/(O_2 \times P_1) - (O_1 \times P_2) \times 100$ %

Where:

- O_1 = molar extinction coefficient (ε) of oxidized Alamar Blue (blue) at 570 nm
- O_2 = ε of oxidized Alamar Blue at 600 nm
- A_1 = Absorbance of treated wells at 570 nm
- A_2 = Absorbance of treated wells at 600 nm
- P_1 = Absorbance of control well (cells with Alamar Blue but no test agent) at 570 nm
- P_2 = Absorbance of control well (cells with Alamar Blue but no test agent) at 600 nm

J. Examining the maximum tolerable number of light illumination cycles *via* cell viability assay

We performed the irradiation protocol to match the timing used during iterative imaging experiments. In the optimized workflow, HeLa cells were irradiated for 90 s, after which they were returned to standard culture conditions inside the incubator for approximately one hour before the next irradiation cycle. This allowed sufficient cellular recovery between successive erasing steps and more closely represents the practical imaging workflow, in which labeling, washing, and imaging steps inherently introduce recovery intervals. In addition, a further optimization was implemented in which the 90 s irradiation dose was delivered as three pulses of 30 s each. This intermittent irradiation strategy was adopted to minimize continuous light exposure and avoid local heating while maintaining efficient photocleavage of the CLEAR linker. Additionally, the number of experimental conditions per plate

was minimized, further reducing environmental stress associated with prolonged handling of the cells outside the incubator. Under these optimized conditions, cells exhibited a significant improvement in viability with minimal signs of toxicity. As shown in Fig. S21, cell viability was 98.66% following 90 s irradiation, 94.03% for 180 s, 95.68% for 270 s, 95.16% for 360 s, and 85.96% for 540 s of irradiation. Importantly, cell viability remained above approximately 85% across the total number of irradiation cycles, remaining well above the commonly accepted 80% viability threshold for live-cell imaging applications (*J. Funct. Biomater.,* 2024, **15**, 382; *J. Funct. Biomater.,* 2014, **5**(2), 43-57). Based on these results, the maximum tolerable number of erasing cycles was determined to be six, corresponding to seven imaging cycles without observable deterioration in cellular health.

To determine the maximum 365 nm light irradiation tolerance, HeLa cells seeded at the same density (density of 12,000 cells per well in 96-well plates) and cultured for 24 h. Later, the cells were exposed to 1, 2, 3, 4 or 6 cycles of 365 nm light irradiation (47.19 mW/cm^2). Each 365 nm light cycle consisted of 90 s exposure (applied as three pulses of 30 s each) followed by a 1 h incubation gap. Following irradiation, cell viability was assessed to evaluate 365 nm light-induced cytotoxicity. After 24 h, cell viability status was checked for using the Alamar Blue assay. For all the cases of Alamar Blue assay, absorbance values at the specified wavelengths (570 nm, 600 nm) were measured and normalized to untreated control cells. The cell viability data were plotted relative to the control group to assess the effects of 365 nm light irradiation and probe incubation on cell survival. The toxicity profile is shown in Fig. S21.

K. Detection of Intracellular Reactive Oxygen Species (ROS)

Intracellular reactive oxygen species (ROS) generation induced by photocleaved product and 365 nm light irradiation was evaluated using the 2′,7′-dichlorofluorescein diacetate (DCFDA) assay. Briefly, 12,000 cells per well were seeded in black, clear-bottom 96-well culture plates and allowed to grow for 24 h under standard culture conditions. Following incubation, cells were washed once with sterile 1× PBS and treated with a solution containing 10 fmol (prepared in 100 µl of complete cell culture medium as 0.1 nM solution) of **2c** (shown in synthesis scheme), prepared in 100 µl of fresh complete culture medium. After 30 min of probe incubation, cells were exposed to 365 nm light irradiation (total duration 90 s, delivered as three 30 s pulses, 47.19 mW/cm^2). Subsequently, cells were returned to the incubator for 1 h, followed by a second 365 nm light irradiation cycle using the same exposure parameters. Control groups included untreated cells and cells subjected to two cycles of 365 nm light irradiation alone, separated by a 1 h interval, without probe treatment. A positive control was established by incubating cells with 0.3% hydrogen peroxide (H_2O_2) for 30 min. For ROS detection,

cells were washed twice with 1× PBS after all treatments. Cells were then incubated with 10 µM DCFDA diluted in phenol red–free, serum-free DMEM for 30 min at 37 °C in the dark. Excess dye was removed by washing twice with 1× PBS, and 100 µL of PBS was added to each well prior to measurement. Fluorescence intensity corresponding to intracellular ROS levels was quantified using a microplate reader with excitation at 485 nm and emission collection at 530 nm. Data were analysed relative to control groups to assess ROS generation resulting from probe incubation and 365 nm light exposure. The ROS profile is shown in Fig. S22.

L. Figures:

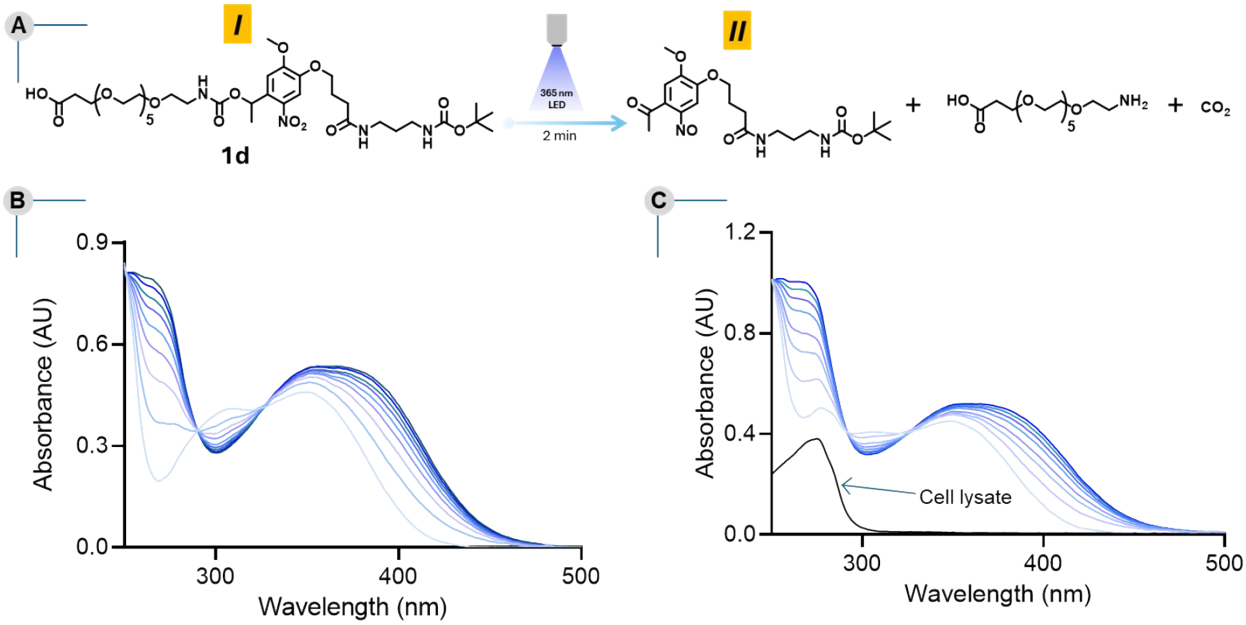

Fig. S1 UV–Vis analysis of the photocleavage pathway and assessment of secondary photoproduct formation. *(A) Photochemical reaction of the o-nitrobenzyl (o-NB)–based photocleavable group upon 365 nm irradiation, showing formation of the nitroso derivative, free amine, and CO_2. Compound 1d, containing the same photocleavable moiety used in CLEAR probes, was used as a model system. (B) UV–Vis absorption spectra of compound* ***1d*** *(100 µM in PBS, 200 µL) recorded during irradiation (0–120 s). The presence of well-defined isosbestic points indicates a clean single-step photocleavage process without detectable intermediate or secondary photoproduct formation. (C) UV–Vis absorption spectra of compound* ***1d*** *recorded under identical irradiation conditions in the presence of HeLa cell lysate (10 µg), showing similar spectral evolution and preserved isosbestic points, indicating that the photocleavage pathway remains unchanged in biologically complex environments.*

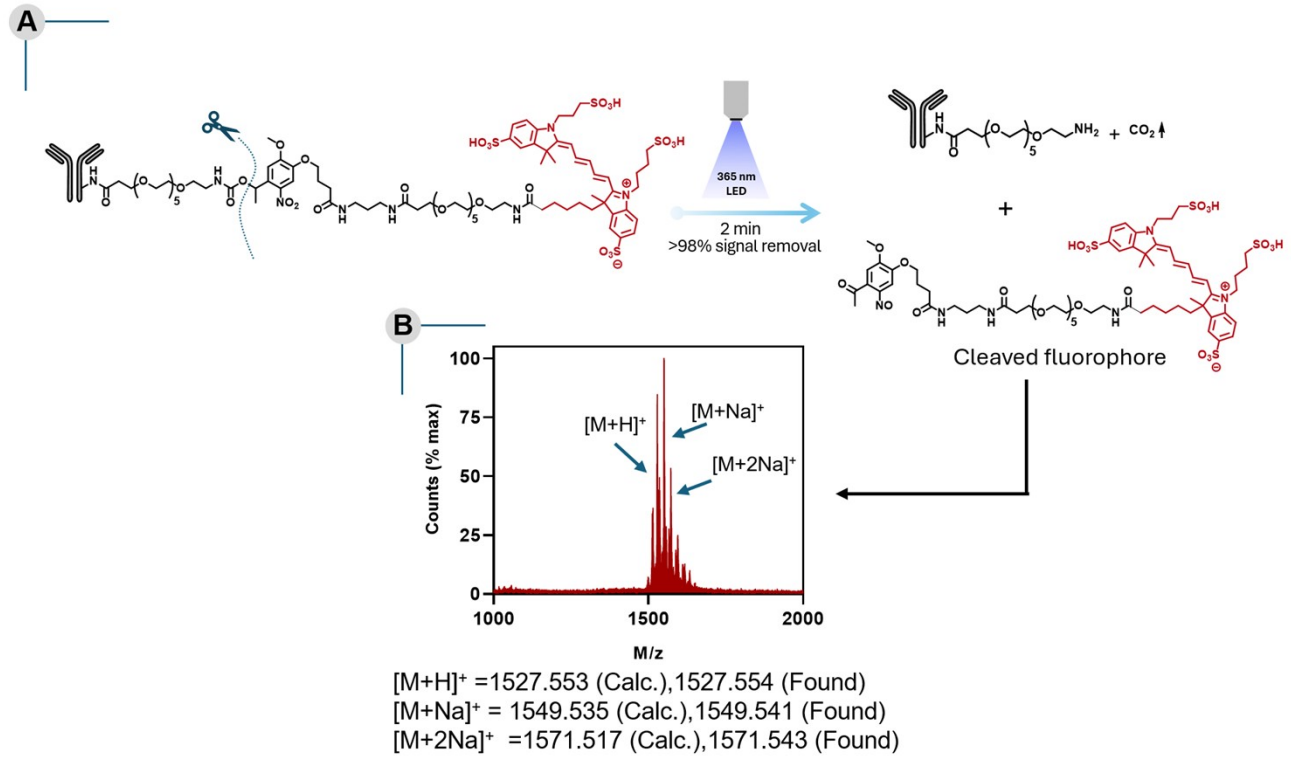

Fig. S2 MALDI-MS analysis of photocleavage products generated from CLEAR probes. *(A) Schematic representation of the photochemical reaction occurring upon 365 nm irradiation of CLEAR-based probes, leading to formation of the antibody fragment bearing a free amine, release of the fluorophore fragment, and evolution of CO_2. (B) MALDI-TOF mass spectrum of the released fluorophore fragment obtained after photocleavage of the CLEAR-647 probe. The calculated and observed masses of the detected species are indicated below the spectrum.*

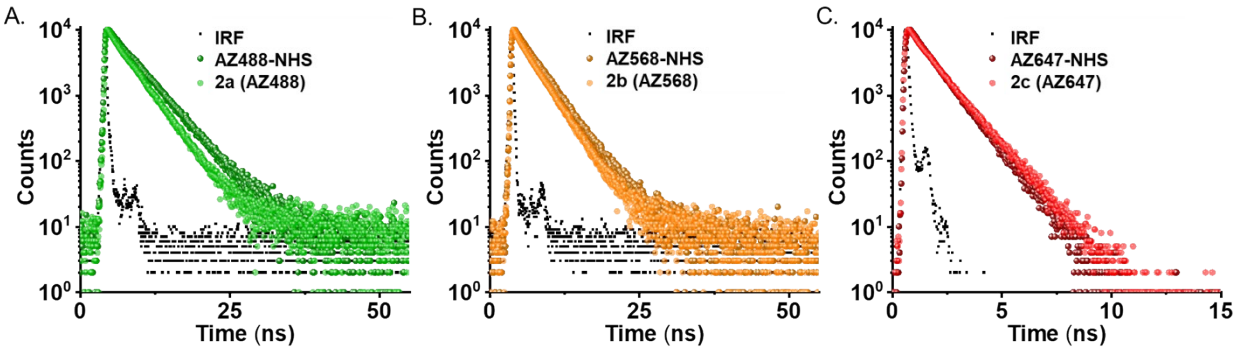

Fig. S3 Fluorescence lifetime decay plots of commercial FL-NHS and their respective photocleavable conjugates at 200 nM concentration in PBS buffer at room temperature. *A) for* ***AZ488-NHS*** *and its photocleavable conjugate* ***2a (AZ488)****, λ_{ex}= 475 nm, λ_{em}= 517 nm. B) for* ***AZ568-NHS*** *and its photocleavable conjugate* ***2b (AZ568)****, λ_{ex}= 510 nm, λ_{em}= 603 nm. C) for* ***AZ647-NHS*** *and its photocleavable conjugate* ***2c (AZ647)****, λ_{ex}= 635 nm, λ_{em}= 671 nm.*

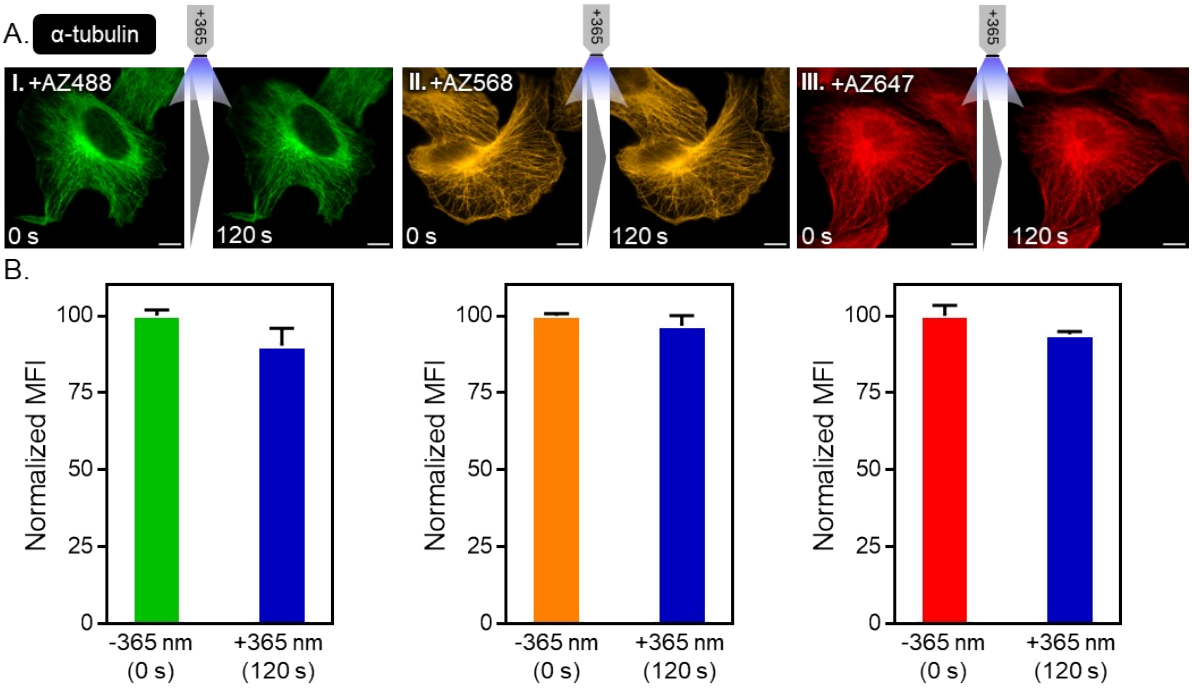

Fig. S4 Effect of 365 nm irradiation on the fluorescence intensity of fluorophore–antibody conjugates lacking a photocleavable linker. *(A) Representative images of α-tubulin in fixed U2OS cells before and after 365 nm irradiation (47.19 mW cm⁻², 2 min). α-Tubulin was visualized by secondary immunostaining using donkey anti-rat antibody–fluorophore conjugates (**AZ488, AZ568, AZ647**) following primary antibody staining. (B) Quantitative plots showing fluorescence intensity changes in the same regions before and after irradiation. Notably, under the same irradiation conditions (365 nm, 47.19 mW cm⁻², 2 min) that produced >98% signal removal in photocleavable linker–based conjugates, no appreciable loss of fluorescence was observed in these control samples. Scale bar: 10 μm.*

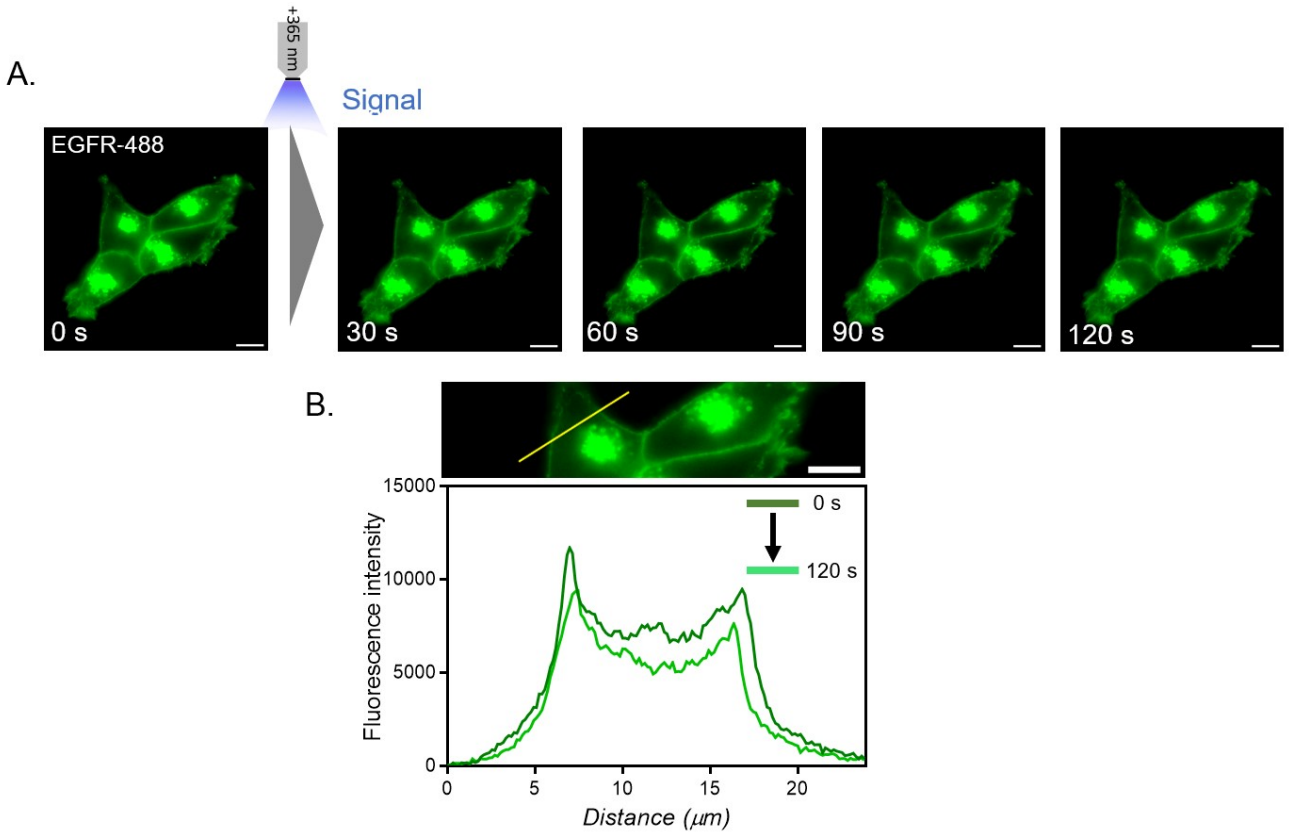

Fig. S5 Effect of 365 nm irradiation on the fluorescence intensity of EGFR labeled via secondary immunostaining with AZ488 lacking a photocleavable moiety. *(A) Representative fluorescence images of EGFR in fixed A431 cells, stained with Cetuximab as the primary antibody and detected using AZ488-conjugated secondary antibodies, acquired at different time points during 365 nm light irradiation (30 s intervals). (B) Fluorescence intensity profiles along the yellow line region before irradiation (0 s) and after 120 s of 365 nm light exposure. Notably, under the same irradiation conditions that produced fluorescence removal in photocleavable linker–based conjugates, EGFR staining with conventional antibody–fluorophore conjugates exhibited no appreciable loss of signal.*

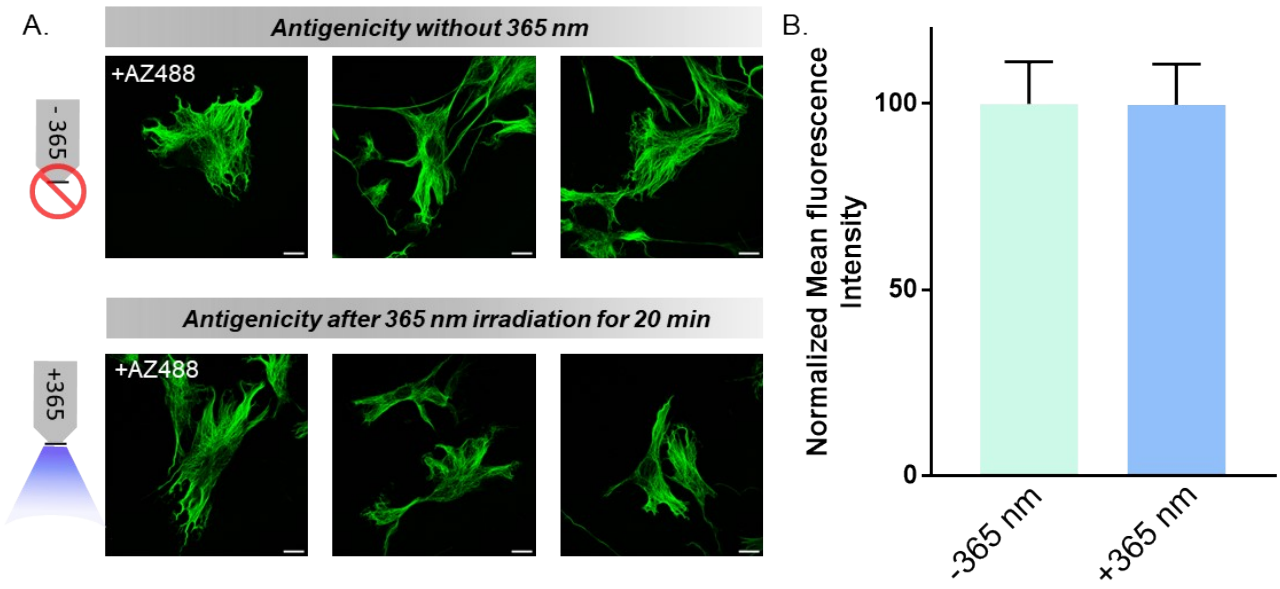

Fig. S6 Assessment of antigenicity retention after continuous 365 nm irradiation. *(A) Confocal images of microtubules in fixed U2OS cells. In the upper panel, α-tubulin was labeled by secondary immunostaining (donkey anti-rat–**AZ488**) without prior irradiation. In the lower panel, α-tubulin was labeled with the same secondary antibody–fluorophore conjugate after 20 min of 365 nm irradiation (47.19 mW cm⁻²). Scale bar: 25 µm. (B) Mean fluorescence intensity plots from selected square regions of stained α-tubulin (N = 10) comparing samples with and without prior 365 nm light exposure.*

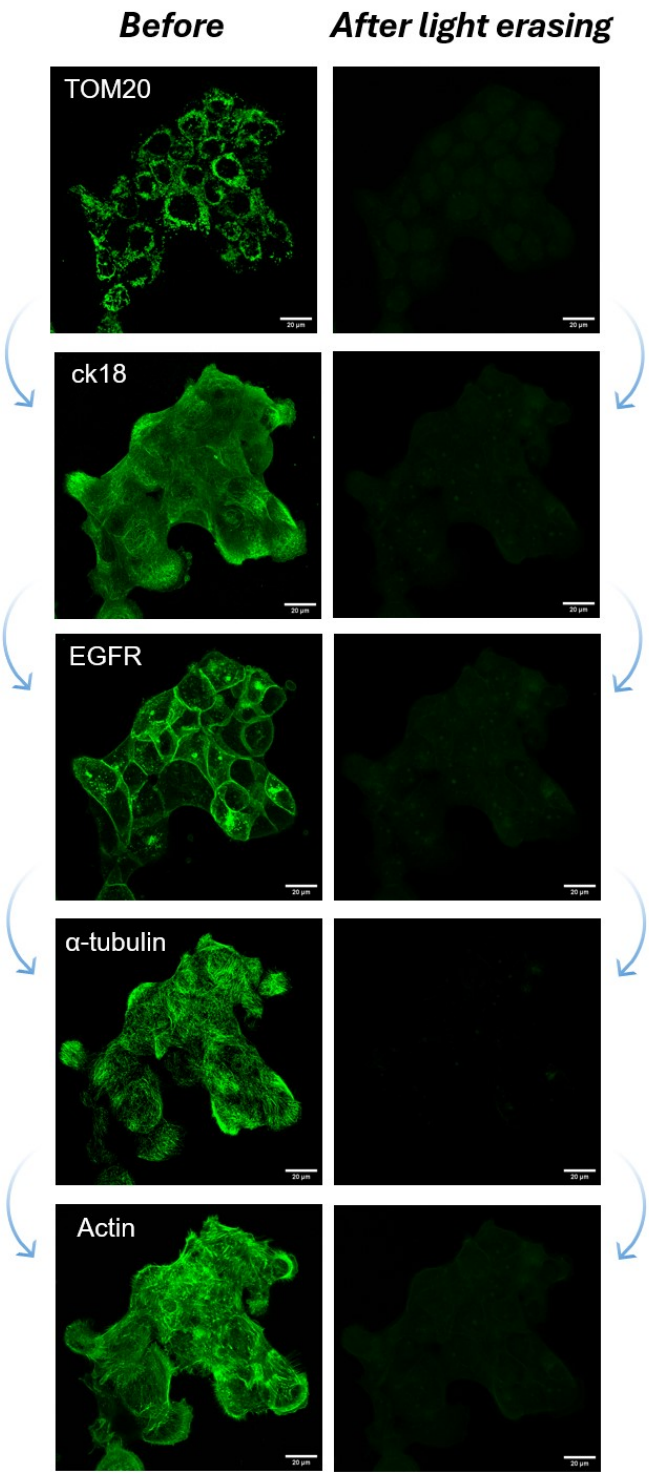

Fig. S7 Effect of photocleavage products on iterative labelling and imaging in fixed A431 cells. *Confocal images of cellular targets (TOM20, CK18, EGFR, α-tubulin, and actin filaments) labelled with CLEAR-488 probes during iterative labelling–imaging–erasing cycles. Images recorded before and after 365 nm irradiation across five consecutive cycles show efficient fluorescence removal with no measurable signal buildup, indicating that photocleavage products do not interfere with subsequent labelling or imaging steps.*

A

CLEAR conjugate	Synthesis date	Evaluation date	Storage duration (PBS, 4 °C)
Donkey anti-rat-CLEAR-647	September, 2022	December, 2025	3 years, 3 months
Donkey anti-rabbit-CLEAR-568	March, 2023	December, 2025	2 years, 9 months
Donkey anti-rabbit-CLEAR-647	March, 2023	December, 2025	2 years, 9 months
Donkey anti-human-CLEAR-488	March, 2023	December, 2025	2 years, 9 months
Donkey anti-rabbit-CLEAR-488	March, 2023	January, 2026	2 years, 10 months

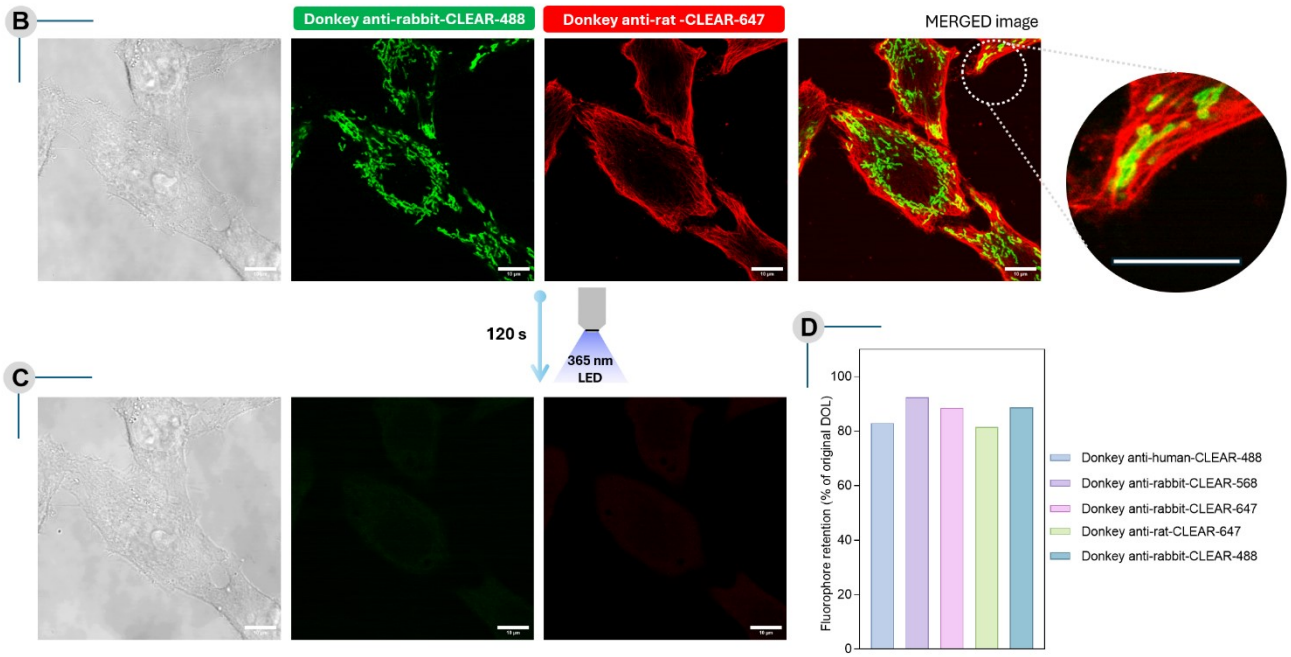

Fig. S8 Long-term storage stability and functional integrity of CLEAR probes. *(A) Synthesis timeline and storage duration of the evaluated CLEAR probes, indicating the dates of synthesis and subsequent evaluation after approximately 2 years 9 months to 3 years 3 months of storage. (B) Brightfield and confocal images of HeLa cells immunostained using aged CLEAR probes. Cells were labeled with primary antibodies against TOM20 (5 µg mL⁻¹) and α-tubulin (5 µg mL⁻¹) for 1 h at room temperature, followed by incubation with the corresponding secondary antibodies, donkey anti-rabbit–CLEAR-488 (5 µg mL⁻¹) and donkey anti-rat–CLEAR-647 (5 µg mL⁻¹), for 1 h at room temperature. The CLEAR probes used were 2 years 9 months and 3 years 3 months old, respectively. (C) Brightfield and confocal images of the same cellular region shown in panel B after 120 s irradiation at 365 nm (47.19 mW cm⁻²), demonstrating efficient light-triggered fluorescence erasure. (D) Evaluation of long-term chemical stability of CLEAR probes based on changes in the degree of labeling (DOL). The plot shows the percentage retention of fluorophores in the indicated CLEAR conjugates after extended storage in PBS at 4 °C.*

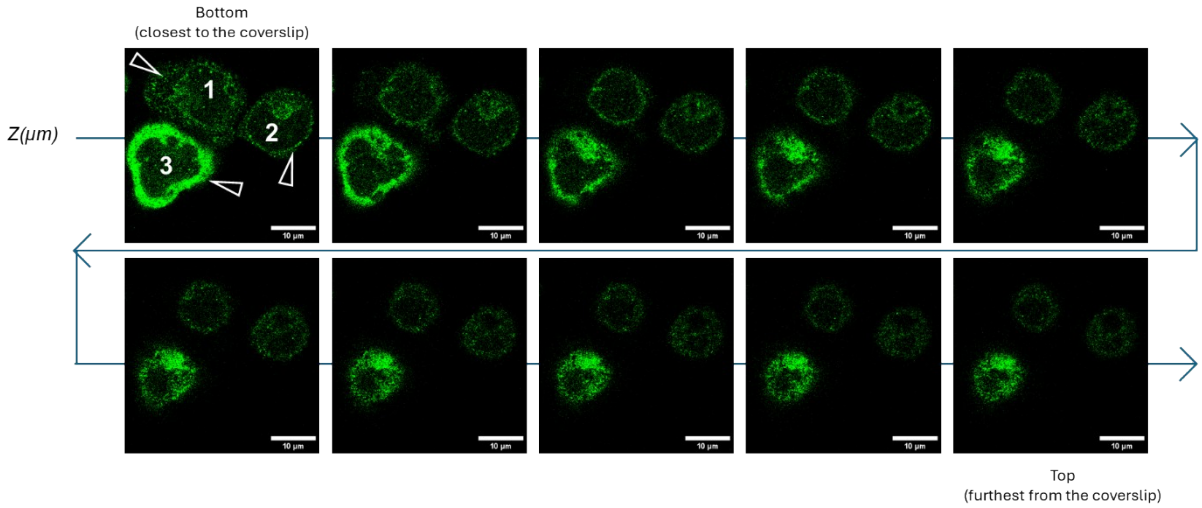

Fig. S9 *The images show the variation in p-ZAP70 signals in Jurkat cells which is an indicative parameter of synapse maturation. Cells 1 and 2 have decayed signal, while Cell 3, being at an earlier stage of synapse maturation, has the brightest visible signal. The arrows in the first image indicate p-ZAP70 signal in the three cells. Scale bar = 10 μm. Separation between z-slices = 0.5 μm.*

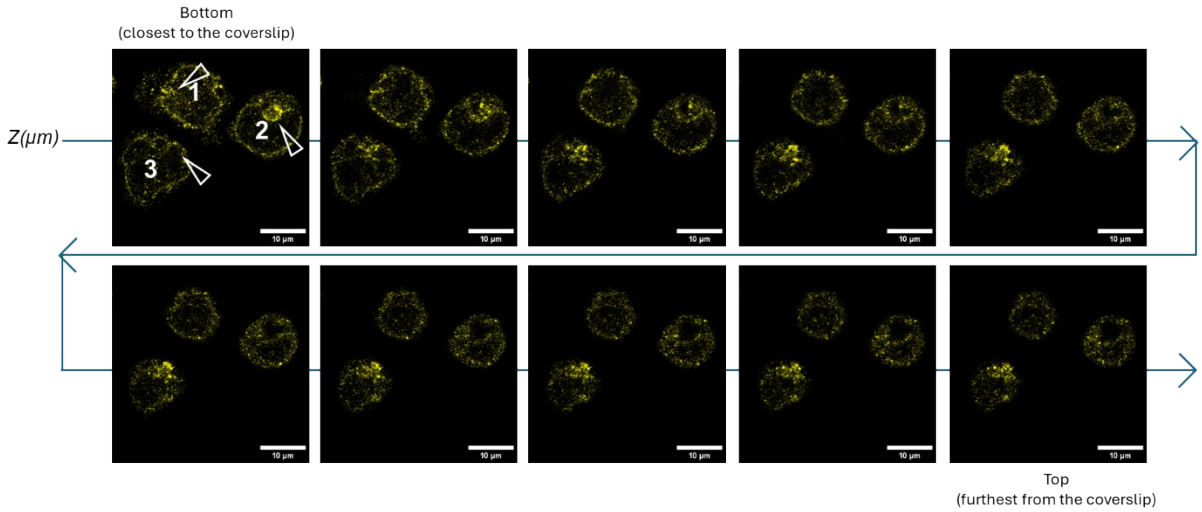

Fig. S10 *These images and arrows in the 1st image show the variations in the distributions of the NUP98 in the nucleus of the three labelled Jurkat cells. At this stage of synapse, the nucleus is typically large, occupying a majority of the cell, and juxtaposed to the synaptic interface, thus the signal from nucleus is unevenly distributed across the synapse and presents as an outline. Arrows in the first image indicate NUP98 signal from the nucleus. Scale bar = 10 μm. Separation between z-slices = 0.5 μm.*

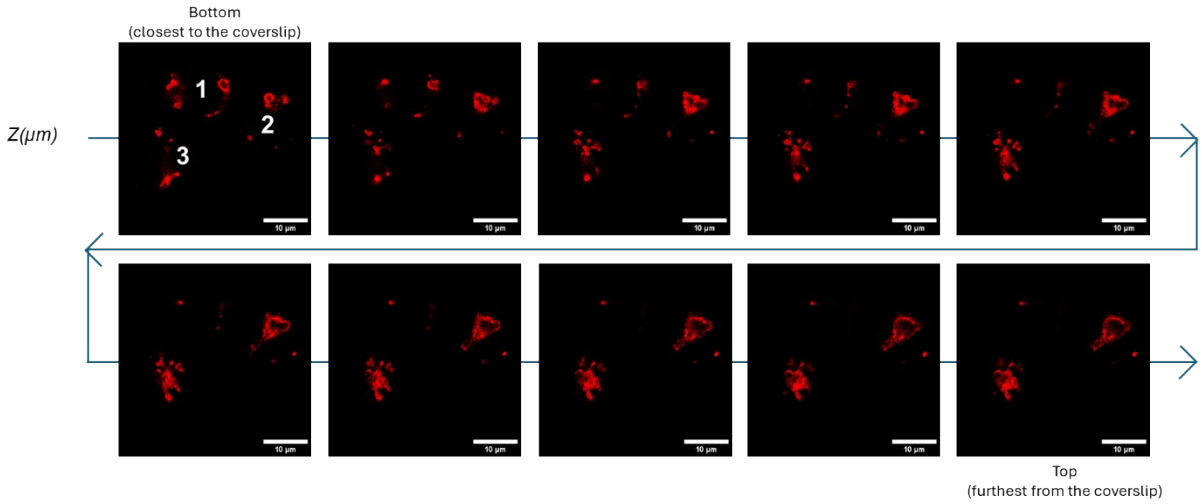

Fig. S11 *The images show the distribution of mitochondria in the three different Jurkat cells upon synapse formation. Since maximum mitochondrial signal accumulation at the synaptic plane occurs after 10-15 minutes of synapse formation, Cells 1, 2, and 3 show a distribution of TOM20 signal across the cell stack. Scale bar = 10 μm. Separation between z-slices = 0.5 μm.*

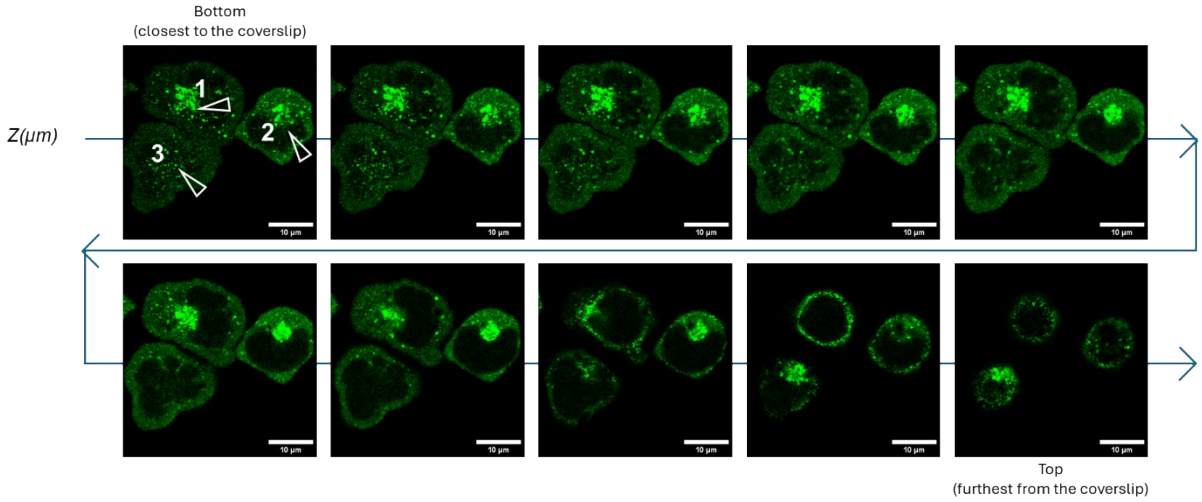

Fig. S12 *The images show different level of synaptic vesicular accumulation in the three Jurkat cells. The vesicular accumulation and targeted trafficking to the cell-substrate interface increases as the synapse matures. This is evident from the images, where cells 1 and 2 show higher centralized clathrin signal intensity at the synapse plane, indicating a more mature synapse compared to cell 3. The arrows in the 1st image indicate the clathrin stains in the three cells. Scale bar = 10 μm. Separation between z-slices = 0.5 μm.*

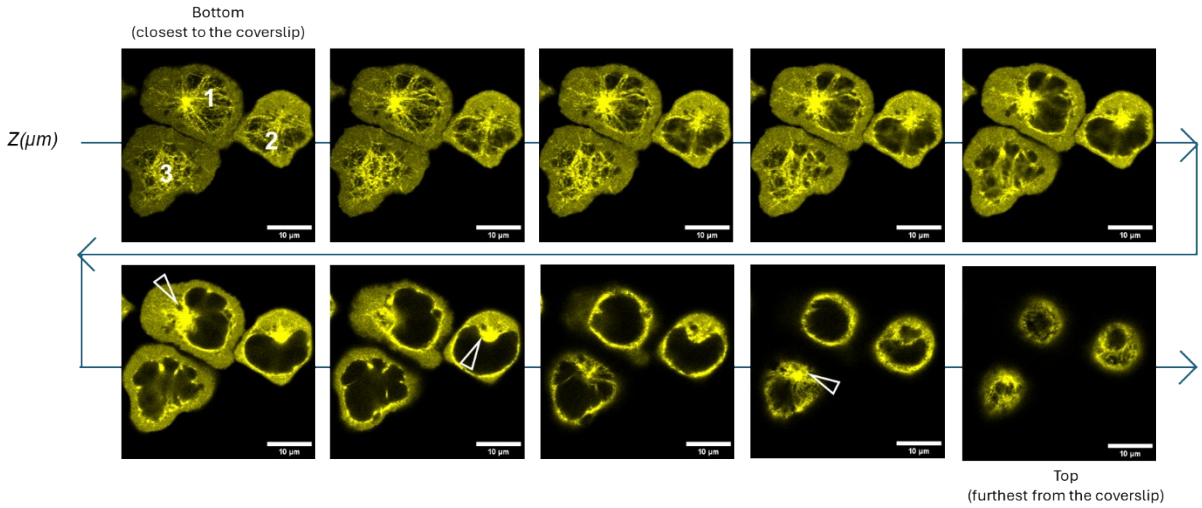

Fig. S13 *The images show differential position of the MTOC in the labelled Jurkat cells via α-tubulin. As the synapse matures, the MTOC is positioned closer to the synapse as is evident from the positions of the MTOC of the three different cells. Cell 3, being the least mature, has its MTOC positioned in higher z-planes. Here, the arrows in 6th, 7th and 9th images indicate differential heights of the highest MTOC signal from the cells 1, 2 & 3 respectively. Scale bar = 10 μm. Separation between z-slices = 0.5 μm.*

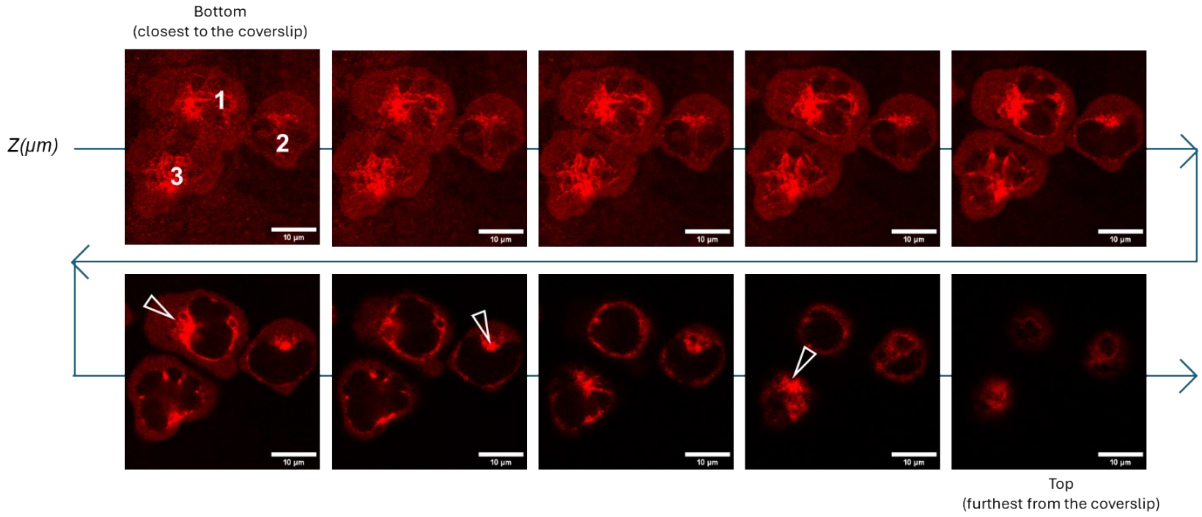

Fig. S14 *The images show differential position of the MTOC in the labelled Jurkat cells via Ac-tubulin. As the synapse matures, the MTOC is positioned closer to the synapse as is evident from the positions of the MTOC of the three different cells. Cell 3, being the least mature, has its MTOC positioned in higher z-planes. Here, the arrows in 6th, 7th and 9th images indicate differential heights of the highest MTOC signal from the cells 1, 2 & 3 respectively. Scale bar = 10 μm. Separation between z-slices = 0.5 μm.*

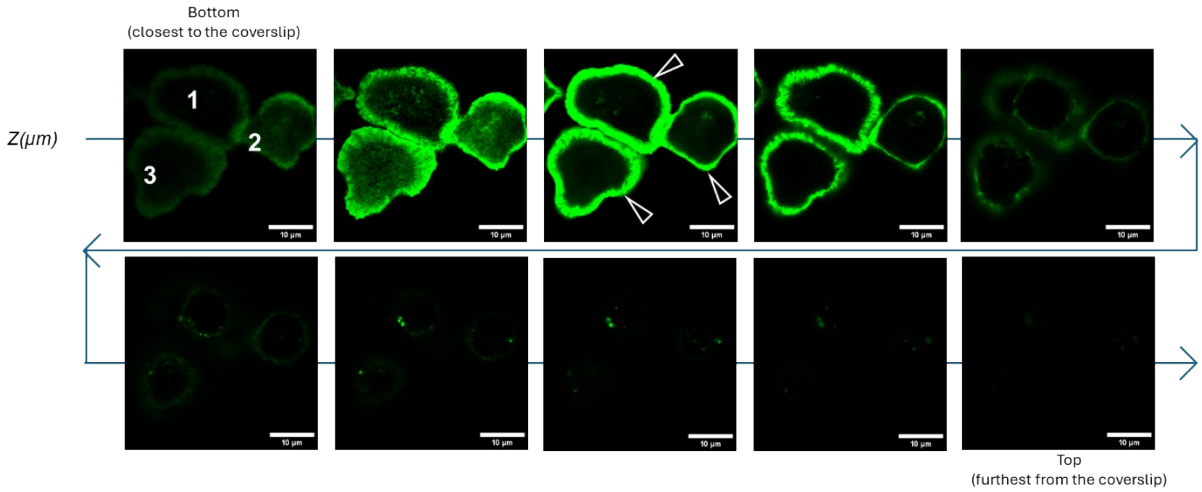

Fig. S15 *The figure shows prominent peripheral actin rings of Jurkat cells upon synapse formation. In all the cells, the actin rings are positioned close to the coverslip in the plane of synapse and are of differential intensity and morphology highlighting the cell-to-cell heterogeneity in the synapse formation and maturation. Arrows in the 3rd image show the prominent actin rings in all three cells. Scale bar = 10 μm. Separation between z-slices = 0.5 μm.*

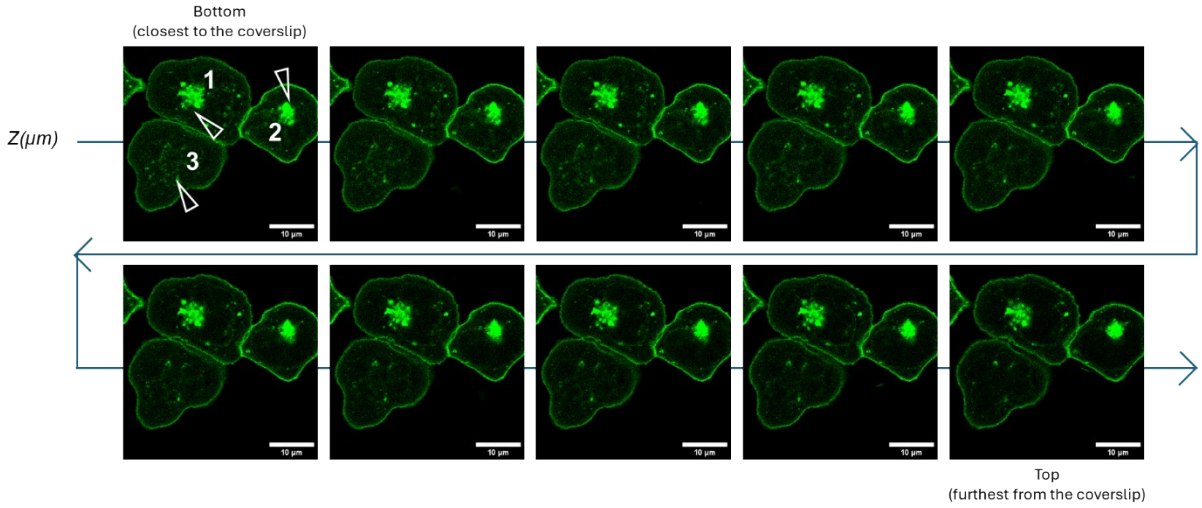

Fig. S16 *The images show variation in WGA-FITC intensity, indicative of vesicular accumulation, in the Jurkat three cells. The vesicular accumulation and targeted trafficking to the cell-substrate interface increases as the synapse matures. This is evident from the images, where cells 1 and 2 show higher centralized staining at the synapse plane, indicating a more mature synapse compared to cell 3. The arrows in the 1st image indicate the WGA-FITC signals in the three cells. Scale bar = 10 μm. Separation between z-slices = 0.5 μm.*

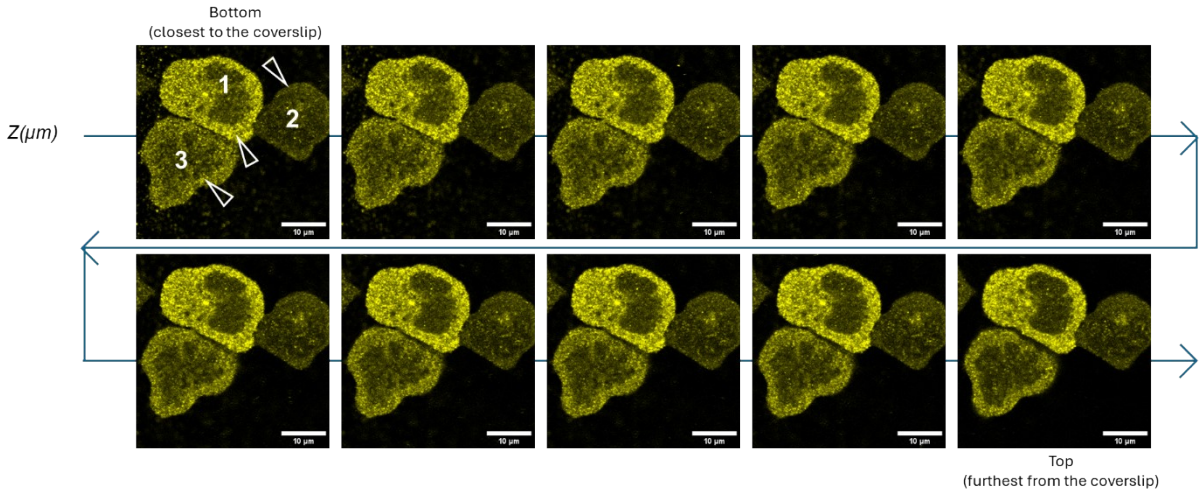

Fig. S17 *The images show paxillin staining in the Jurkat cells and is indicative of focal points in the adhesion ring which lies at the cell-substrate interface. The differential intensity of the paxillin in the three cells is indicative of variability in the stability of adhesion ring. The arrows in the first image highlights this prominent peripheral adhesion ring which varies in stability from cell to cell depending on synapse stage. Scale bar = 10 μm. Separation between z-slices = 0.5 μm.*

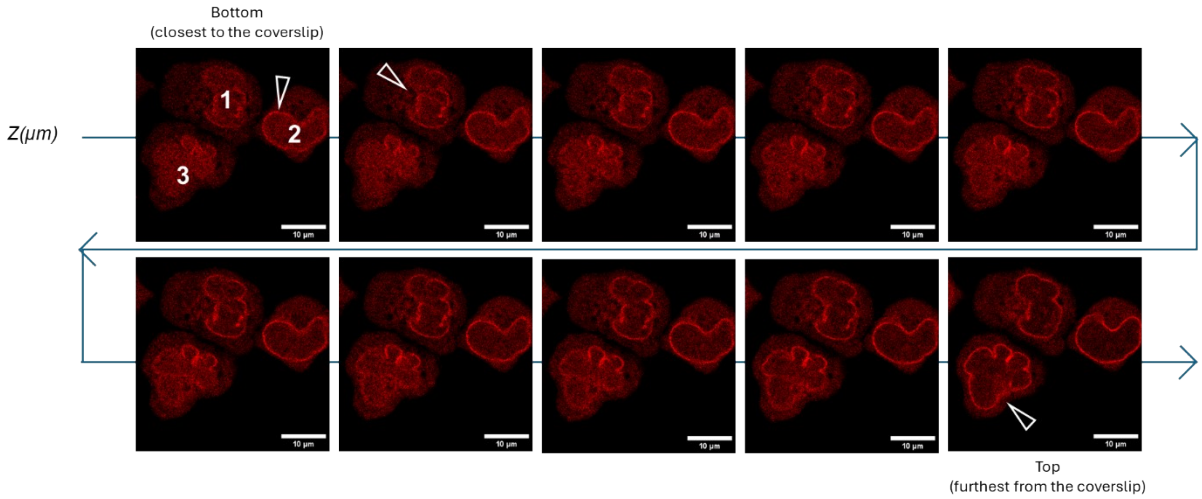

Fig. S18 *The images show the differential positioning of the nuclear envelope marker, lamin B1 of Jurkat cells with respect to the extent of synapse maturation. The arrows in the 1st ,2nd and the 10th images show the nuclear envelope of the cell 1,2 and 3 respectively. The cells 1 and 2 have their nuclear envelope positioned more towards the coverslip relative to that of the less matured cell 3. Scale bar = 10 μm. Separation between slices = 0.5 μm.*

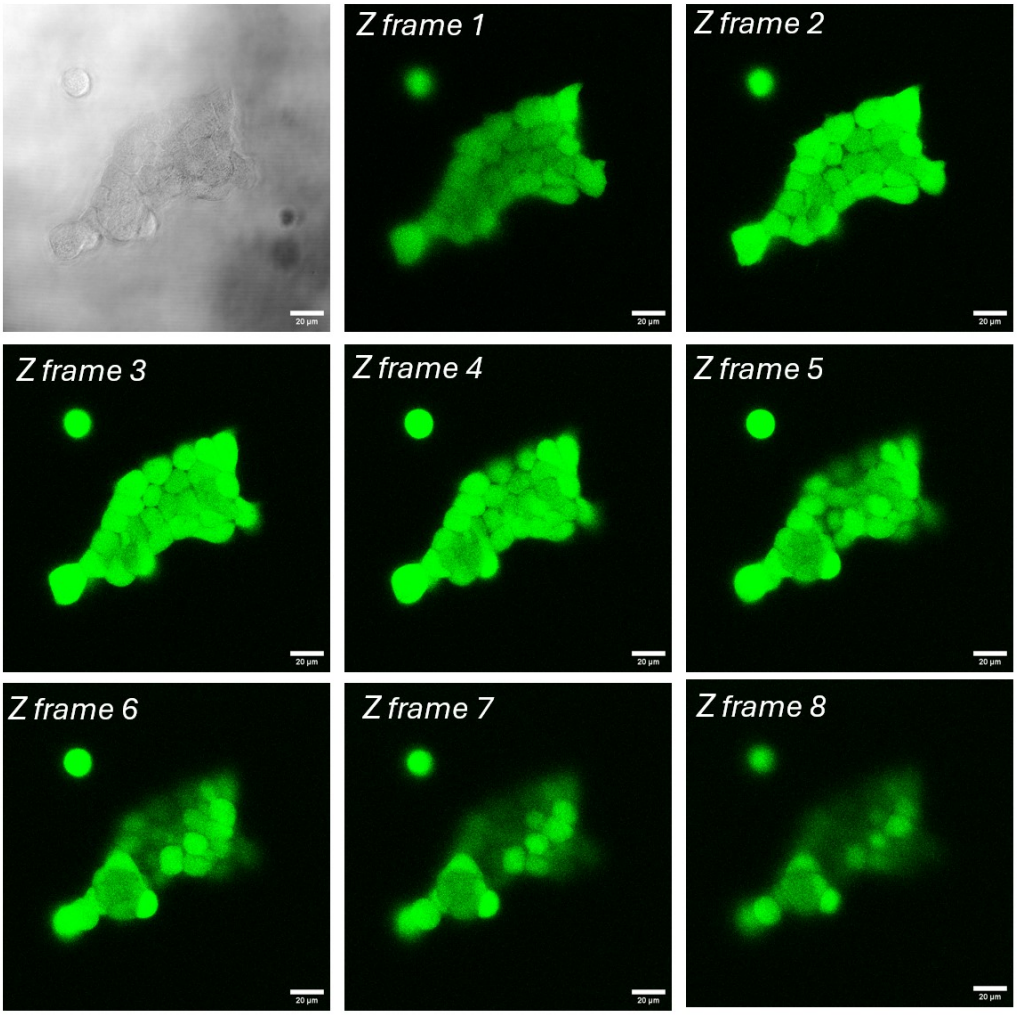

Fig.19 *Z-stack confocal imaging of live A431 cells following 365 nm light irradiation. Brightfield and confocal images of live A431 cells stained with Calcein AM after 180 s irradiation at 365 nm. Confocal images correspond to different z-planes within the same region of interest, where increasing frame numbers indicate higher focal positions along the z-axis. Cells appearing weakly fluorescent in a single imaging plane exhibit strong cytosolic fluorescence at the appropriate focal depth, confirming that intensity variations arise from imaging-plane effects rather than reduced cell viability or staining efficiency. Scale bar = 20 µm.*

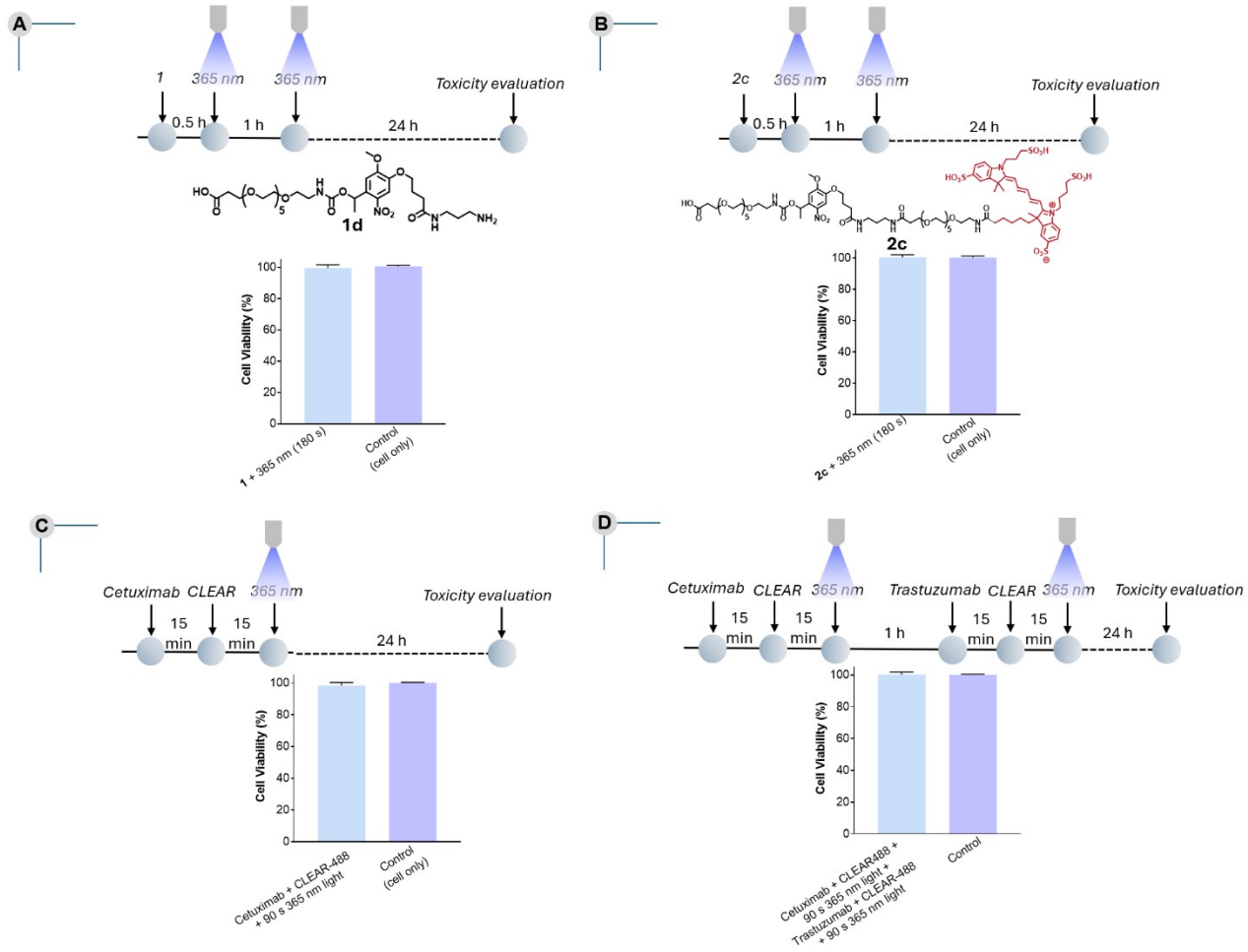

Fig. S20 Evaluation of cellular toxicity associated with photocleavage products and light exposure on HeLa cells. *(A,B) Experimental timelines and corresponding cell viability measurements for assessing the toxicity of photocleavage products generated from small-molecule surrogate compounds 1 and 2c upon 365 nm irradiation, representing the intrinsic effect of released photoproducts. (C) Experimental timeline and corresponding cell viability profile following antibody-based labelling using cetuximab and donkey anti-human CLEAR-488, followed by 365 nm irradiation to simulate a single signal-erasing step under imaging-relevant conditions. (D) Experimental timeline and corresponding cell viability profile following two consecutive rounds of immunostaining and irradiation, mimicking iterative labelling–imaging–erasing cycles. The first cycle involved cetuximab followed by CLEAR-488 labelling and irradiation, and the second cycle involved trastuzumab followed by CLEAR-488 labelling and irradiation. Cell viability was assessed 24 h after irradiation in all cases.*

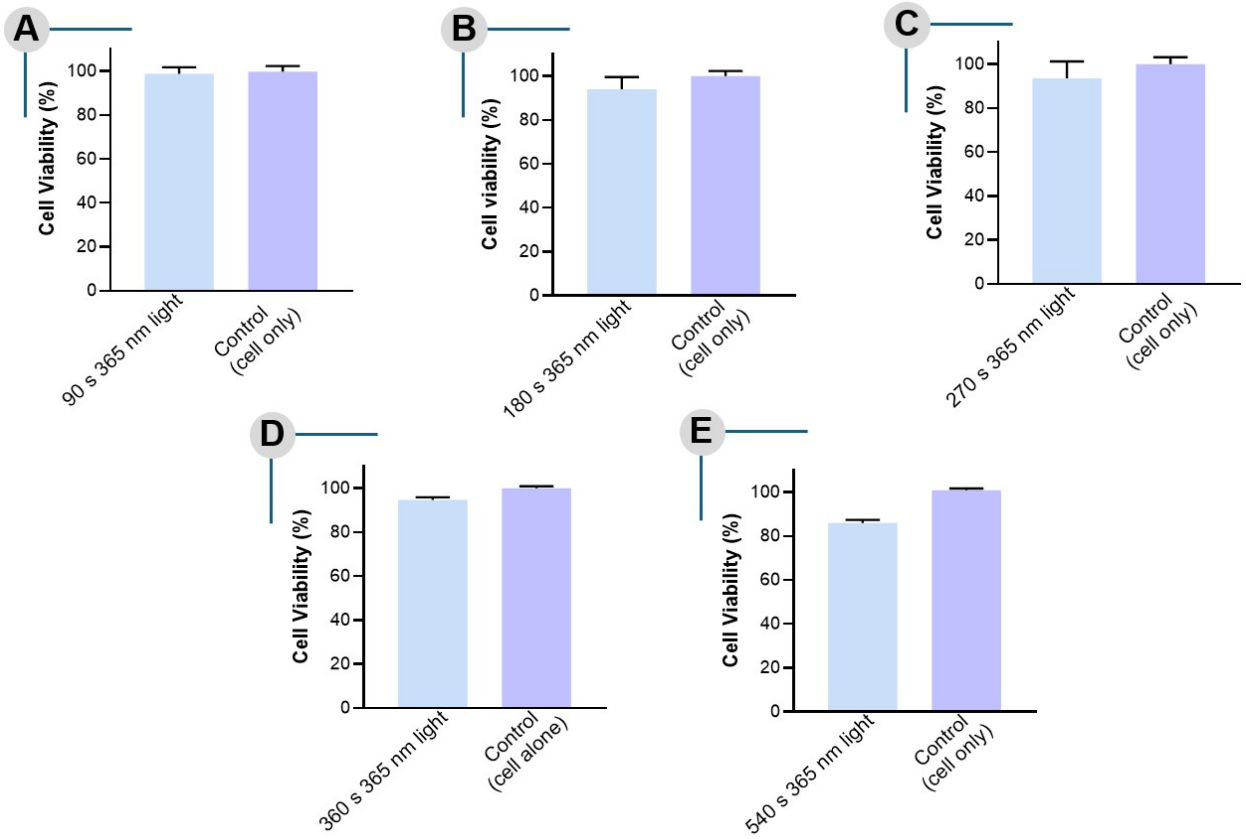

Fig. S21 *Evaluation of cell viability of under repeated 365 nm irradiation conditions. Cell viability of HeLa cells following irradiation at 365 nm for increasing total exposure times of 90 s, 180 s, 270 s, 360 s, and 540 s, corresponding to multiple illumination cycles used during iterative imaging experiments. Panels (A–E) show the respective viability profiles under optimized irradiation conditions, in which light exposure was delivered in intermittent pulses with recovery intervals between cycles. The results demonstrate high cellular viability across repeated irradiation cycles, indicating minimal phototoxicity under imaging-relevant conditions.*

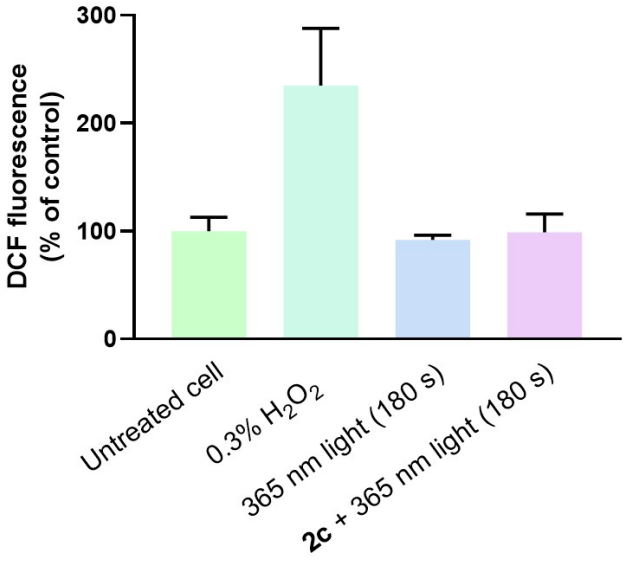

Fig. S22 Evaluation of intracellular ROS generation under optimized irradiation conditions. *ROS levels in HeLa cells were assessed using a DCFDA assay under different conditions: untreated control, 0.3% H_2O_2 (positive control), 365 nm irradiation for 180 s, and precursor* ***2c*** *followed by 365 nm irradiation. ROS levels are reported as relative DCF fluorescence intensity normalized to untreated cells. While H_2O_2 treatment resulted in elevated ROS generation, cells exposed to irradiation alone or precursor* ***2c*** *plus irradiation showed ROS levels comparable to control cells, indicating negligible oxidative stress under optimized CLEAR imaging conditions.*

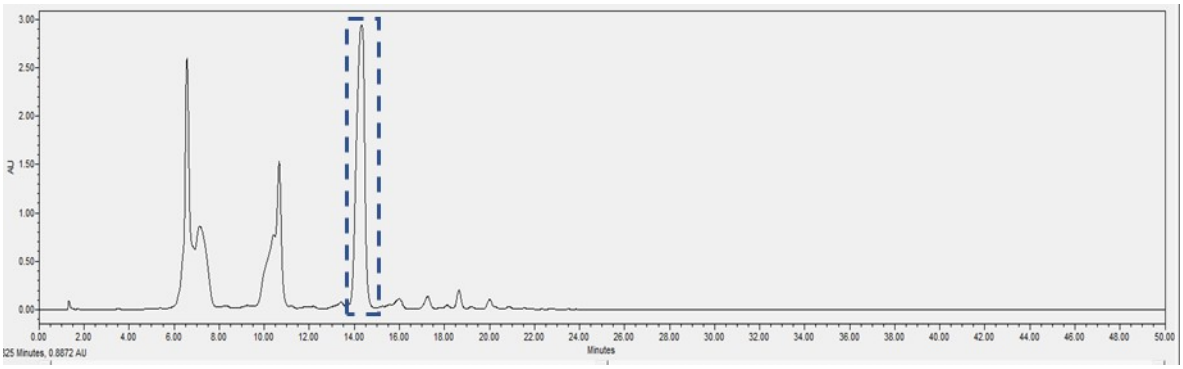

Fig. S23 *HPLC chromatogram of the compound 1b*

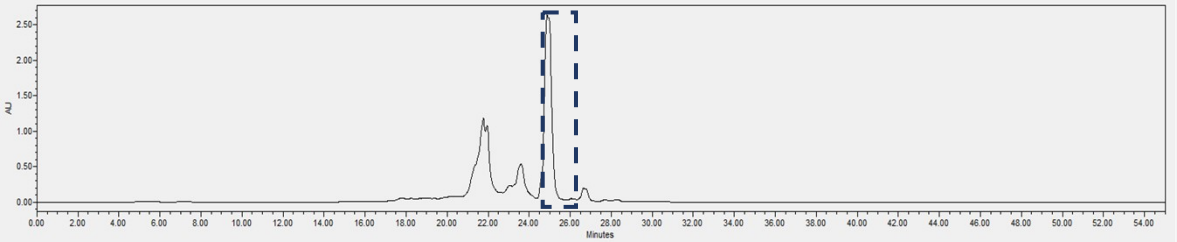

Fig. S24 *HPLC chromatogram of compound 1c*

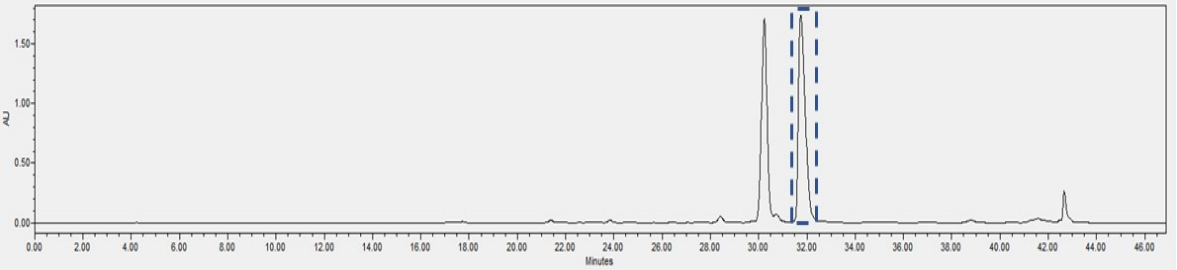

Fig. S25 *HPLC chromatogram of compound 1d*

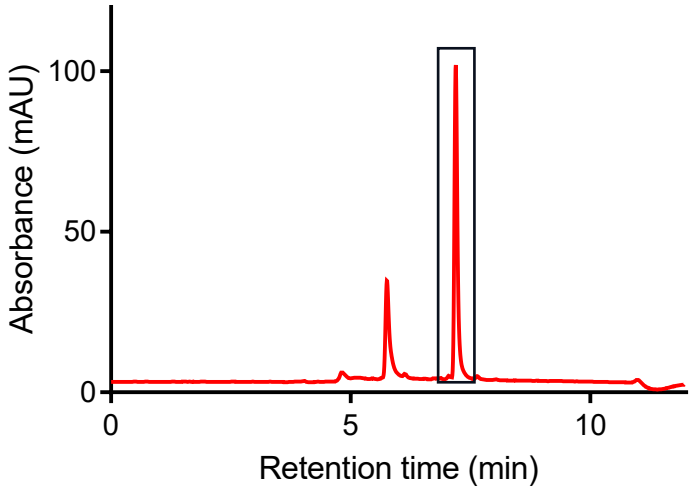

Fig. S26 *HPLC chromatogram of AZ488-PEG-COOH*

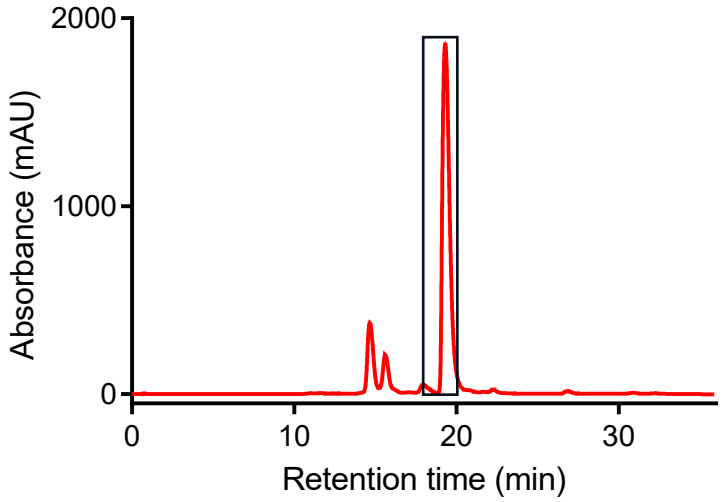

Fig S27 *HPLC chromatogram of AZ488-PEG-NHS*

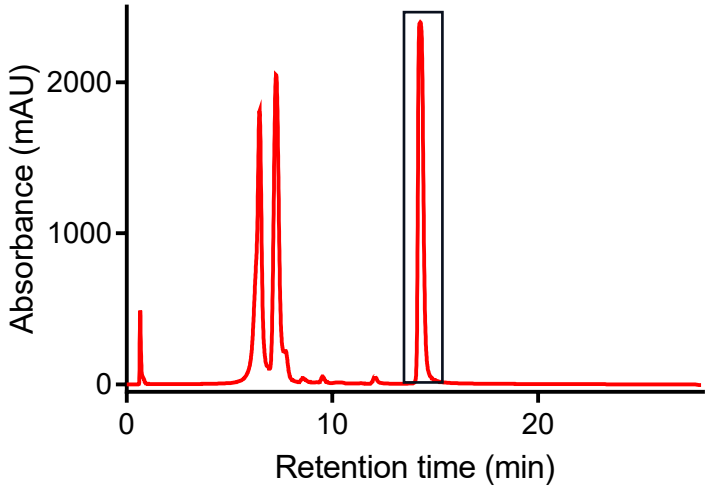

Fig. S28 *HPLC chromatogram of* ***2a (AZ488)***

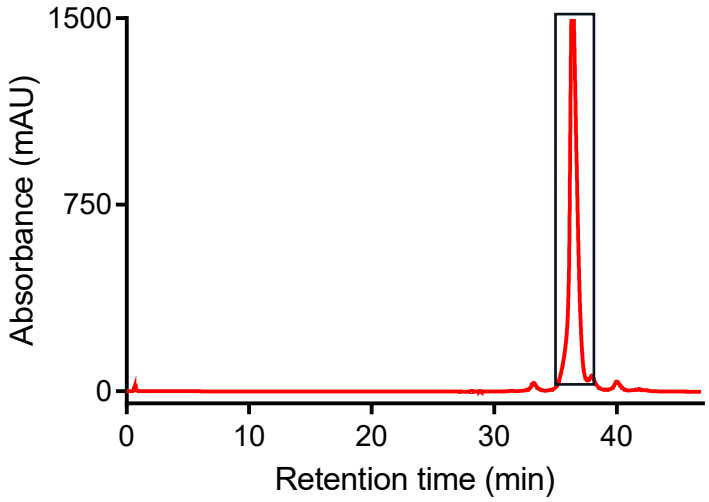

Fig. S29 *HPLC chromatogram of 3**a** **(AZ488)***

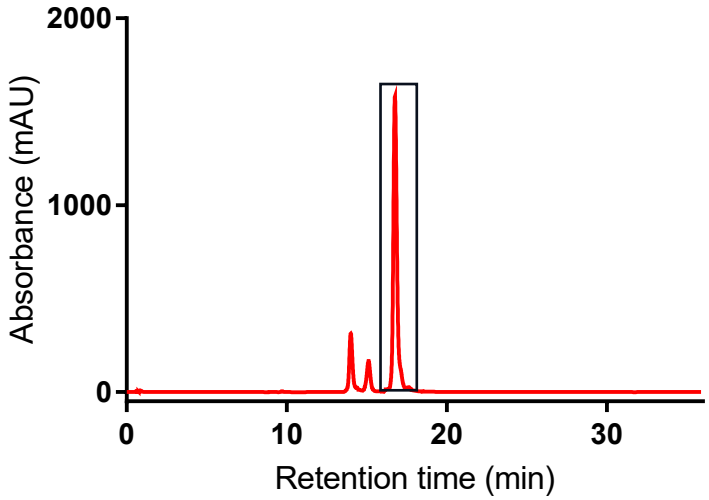

Fig. S30 *HPLC chromatogram of* ***Phalloidin-CLEAR-488***

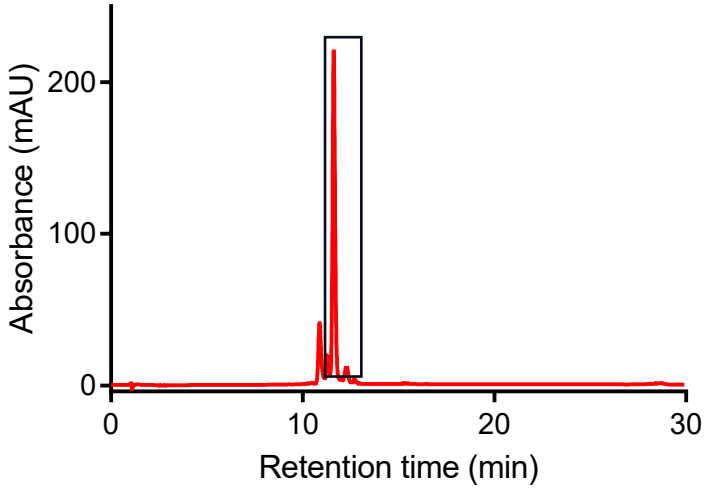

Fig. S31 *HPLC chromatogram of* ***AZ568-PEG-COOH***

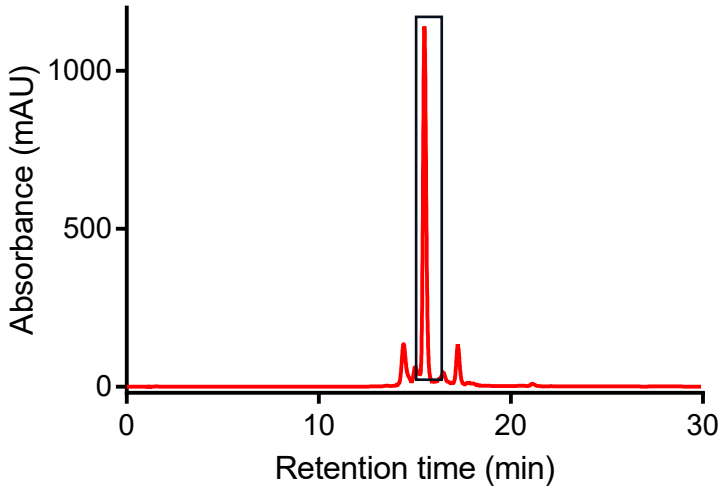

Fig. S32 *HPLC chromatogram of* ***AZ568-PEG-NHS***

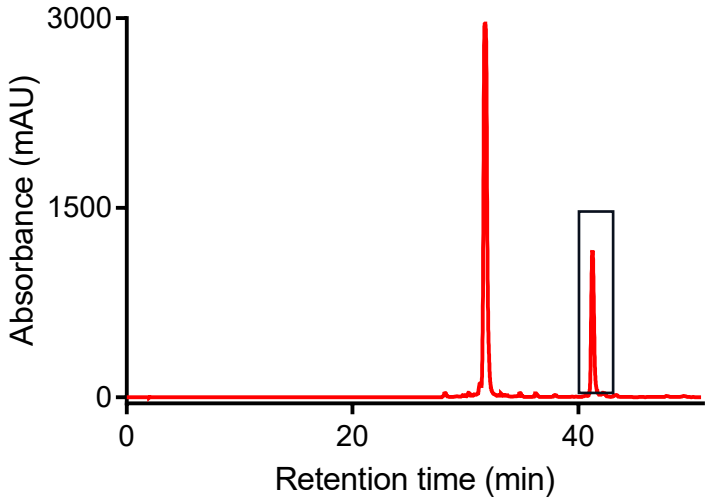

Fig. S33 *HPLC chromatogram of* ***2b (AZ568)***

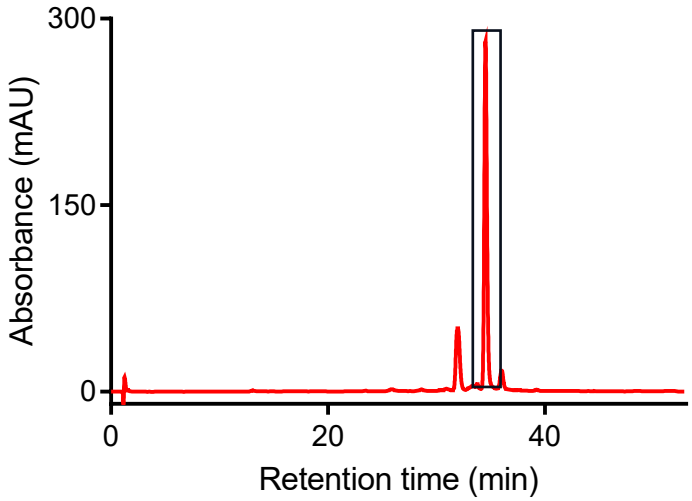

Fig. S34 *HPLC chromatogram of* ***3b (AZ568)***

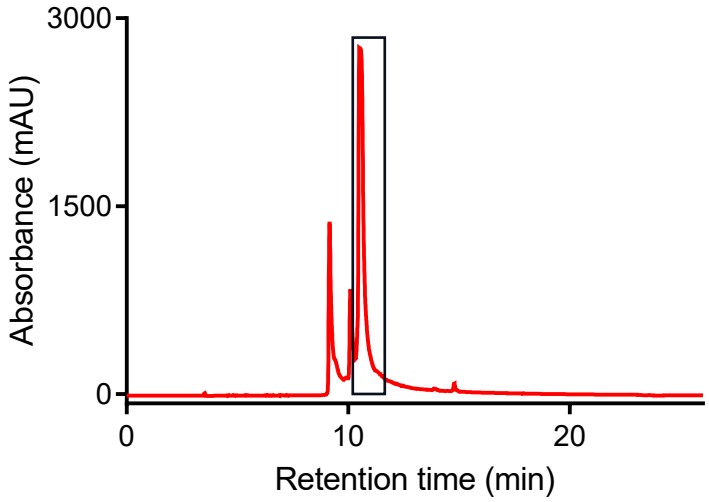

Fig. S35 *HPLC chromatogram of* ***AZ647-PEG-COOH***

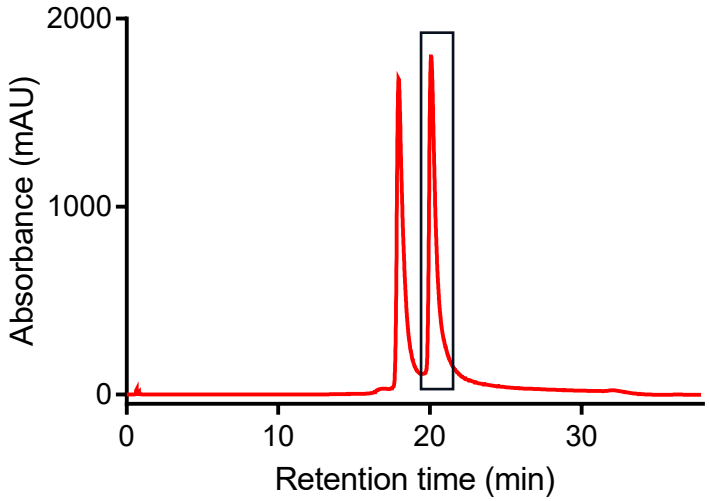

Fig. S36 *HPLC chromatogram of* ***AZ647-PEG-NHS***

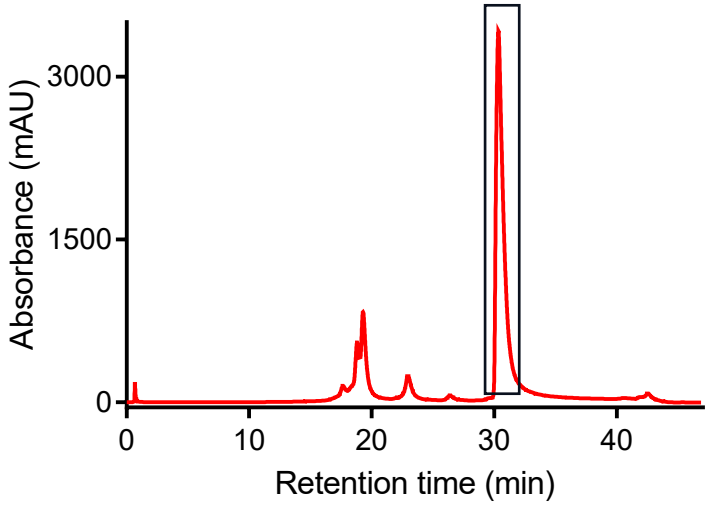

Fig. S37** HPLC chromatogram of **2c (AZ647)

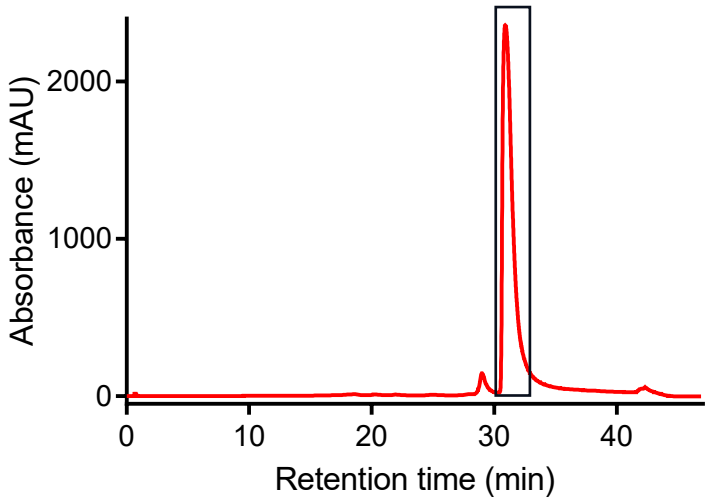

Fig. S38** HPLC chromatogram of **3c (AZ647)

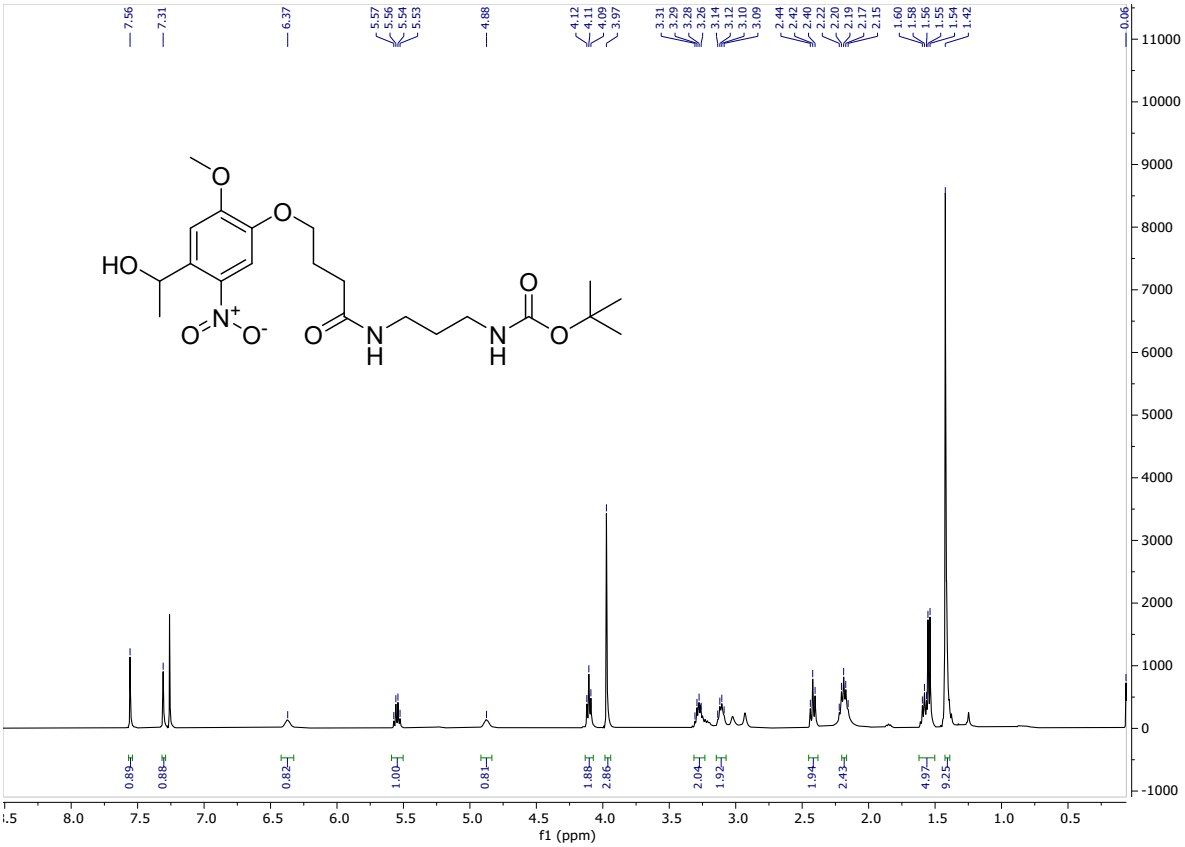

Fig. S39 *^{1}H NMR spectrum of compound 1b*

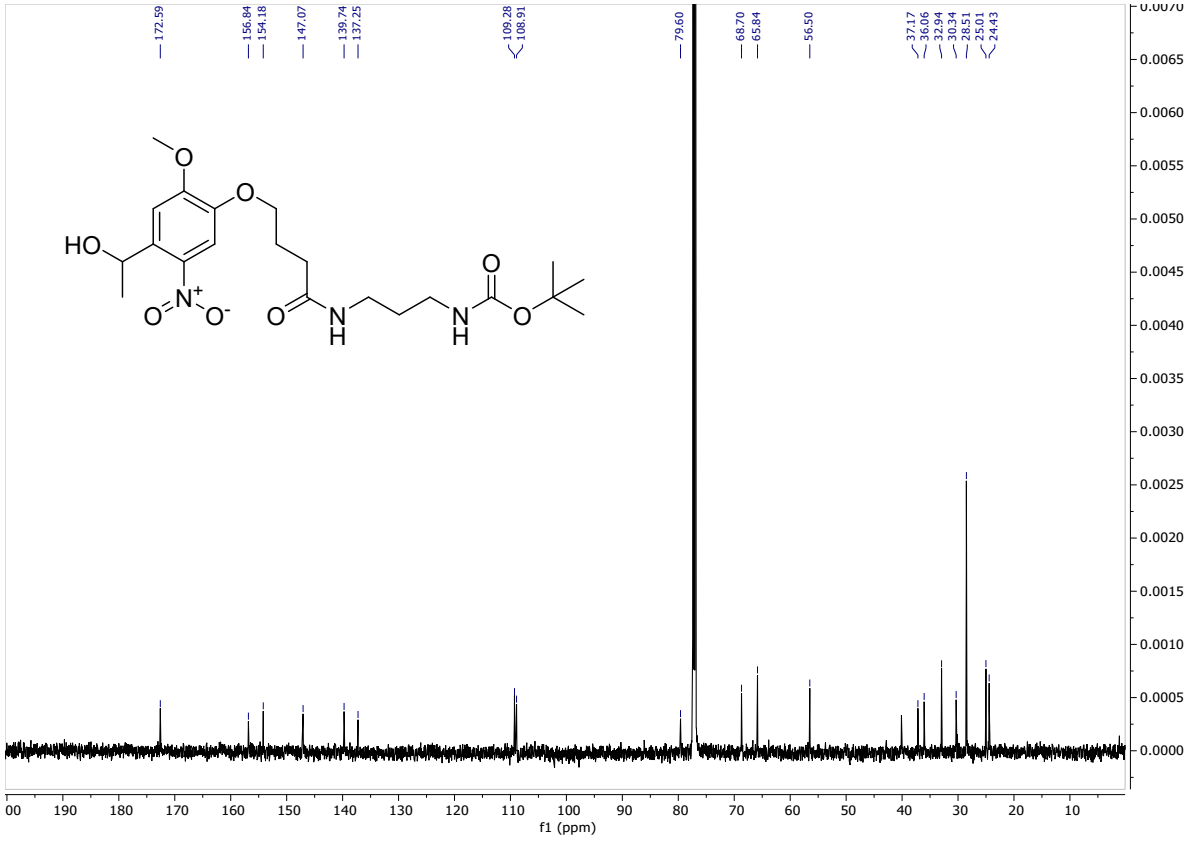

Fig. S40 *^{13}C NMR spectrum of compound 1b*

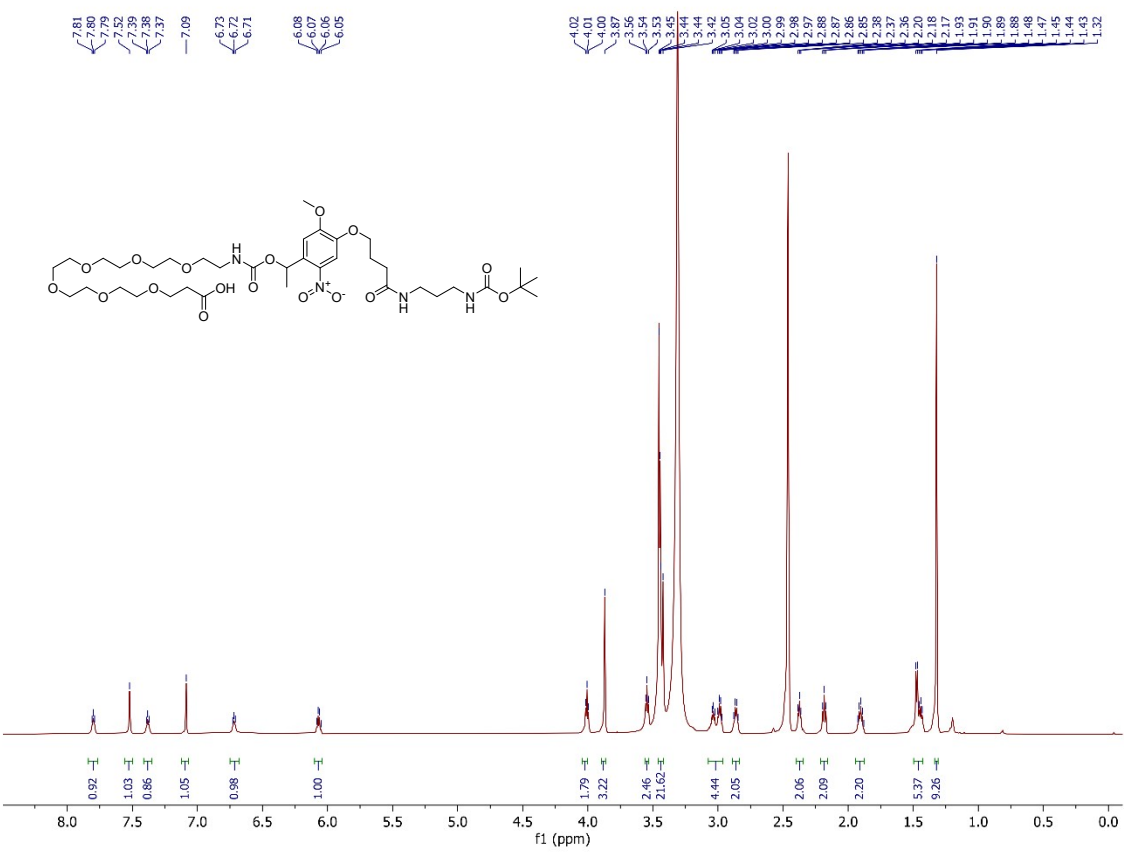

Fig. S41 *^{1}H NMR spectrum of compound 1d*

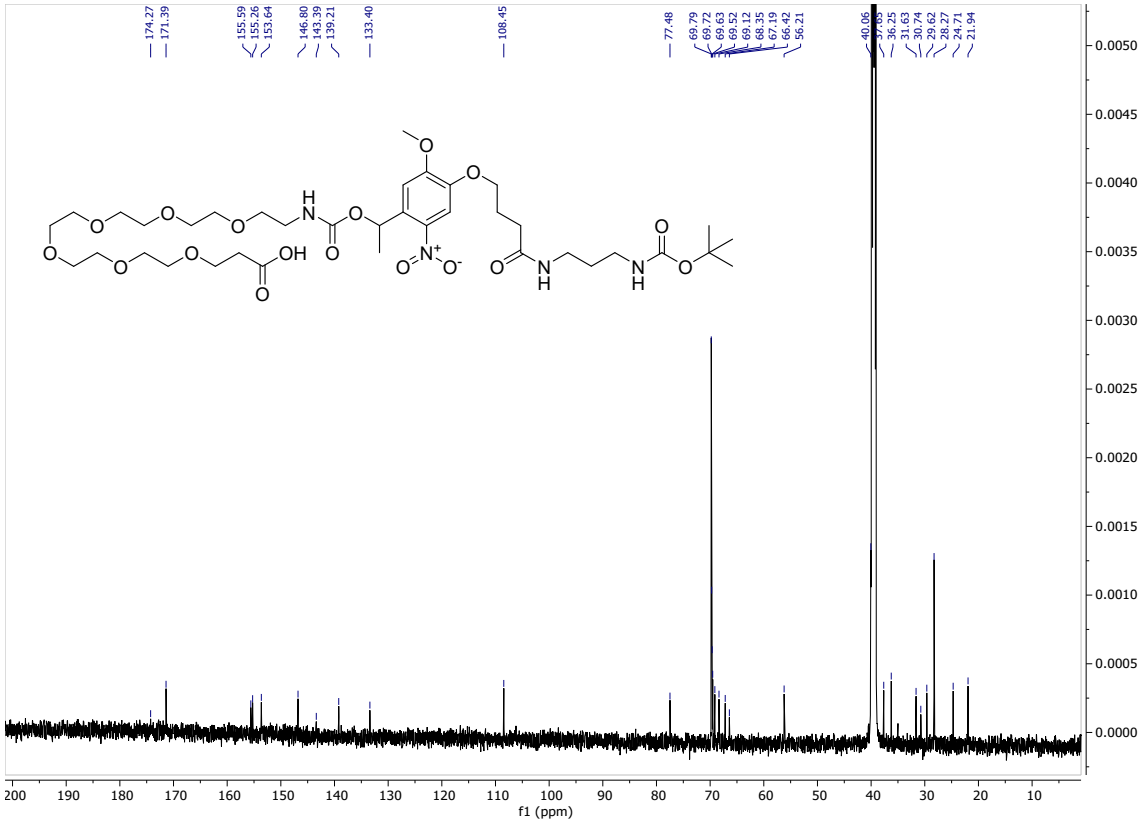

Fig. S42 *^{13}C NMR spectrum of compound 1d*

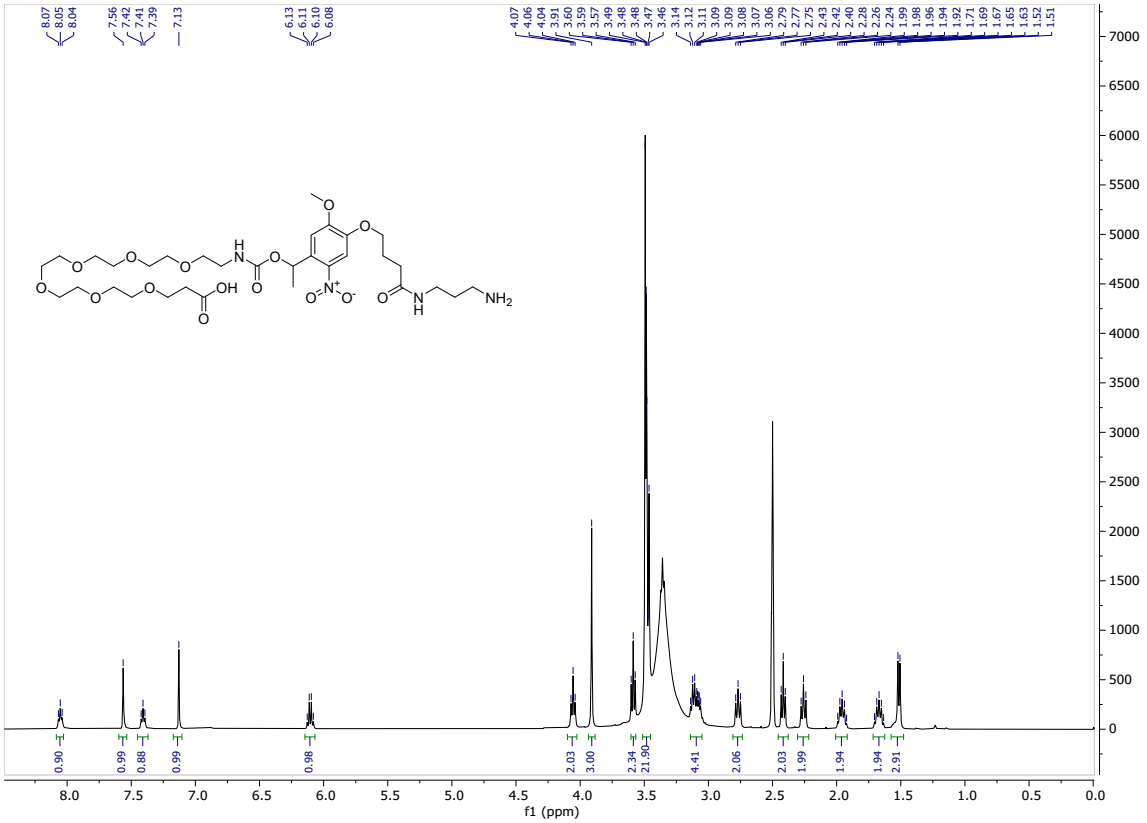

Fig. S43 *^{1}H NMR spectrum of compound 1*

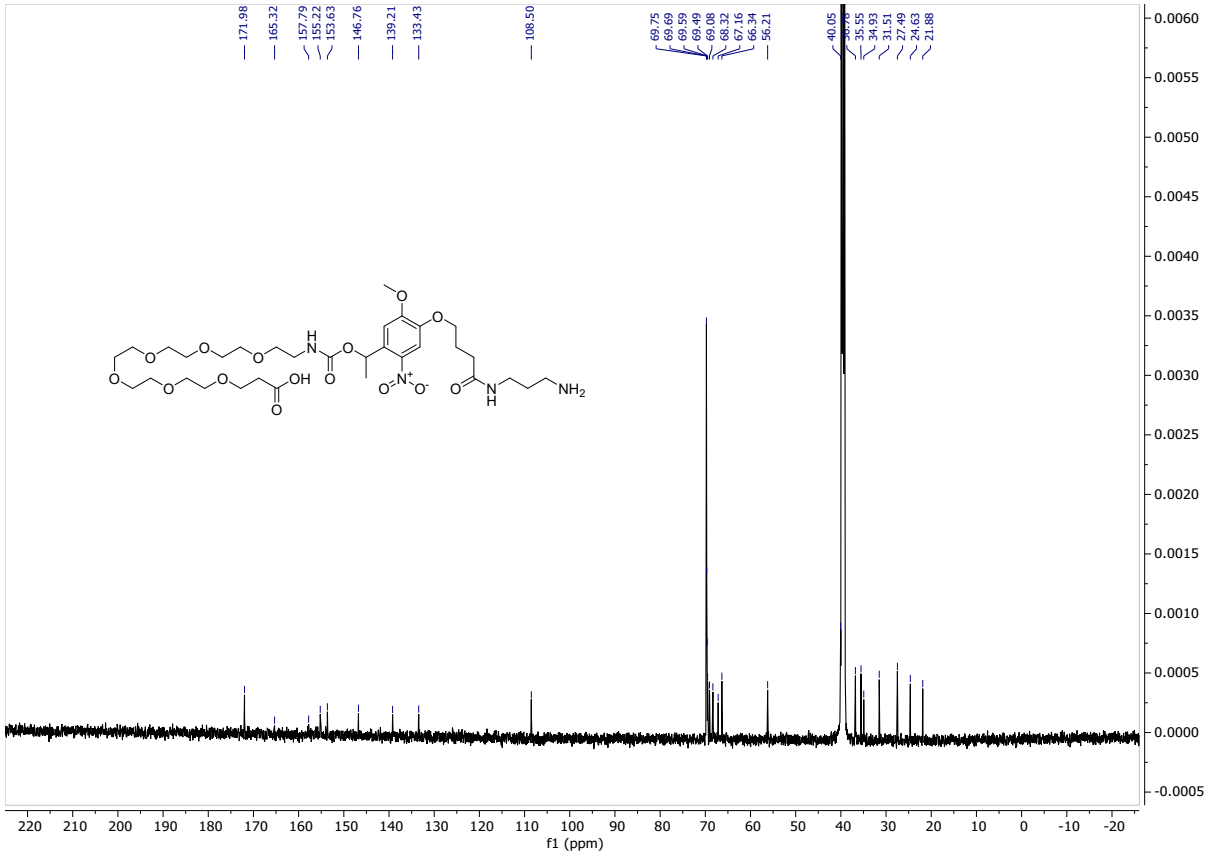

Fig. S44 *^{13}C NMR spectrum of compound 1*

References:

1. C. P. Holmes, *J. Org. Chem.* **1997**, *62,* 2370-2380.